

MODELING THE REMOVAL OF SULFUR DIOXIDE AND NITROGEN OXIDES
FROM FLUE GASES USING COMBINED PLASMA AND OPTICAL PROCESSING

BY

JEANNE HICKMAN BALBACH

A.B., University of Illinois, 1970

THESIS

Submitted in partial fulfillment of the requirements
for the degree of Master of Science in Electrical Engineering
in the Graduate College of the
University of Illinois at Urbana-Champaign, 1991

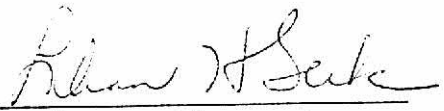
Urbana, Illinois

UNIVERSITY OF ILLINOIS AT URBANA-CHAMPAIGN
GRADUATE COLLEGE DEPARTMENTAL FORMAT APPROVAL

THIS IS TO CERTIFY THAT THE FORMAT AND QUALITY OF PRESENTATION OF THE THESIS
SUBMITTED BY JEANNE HICKMAN BALBACH AS ONE OF THE
REQUIREMENTS FOR THE DEGREE OF MASTER OF SCIENCE
ARE ACCEPTABLE TO THE DEPARTMENT OF ELECTRICAL AND COMPUTER ENGINEERING
Full Name of Department, Division or Unit

8 October 1990

Date of Approval


Departmental Representative

UNIVERSITY OF ILLINOIS AT URBANA-CHAMPAIGN

THE GRADUATE COLLEGE

SEPTEMBER 1990

WE HEREBY RECOMMEND THAT THE THESIS BY

JEANNE HICKMAN BALBACH

ENTITLED MODELING THE REMOVAL OF SULFUR OXIDE AND NITROGEN OXIDES

FROM FLUE GASES USING COMBINED PLASMA AND OPTICAL PROCESSING

BE ACCEPTED IN PARTIAL FULFILLMENT OF THE REQUIREMENTS FOR

THE DEGREE OF MASTER OF SCIENCE IN ELECTRICAL ENGINEERING

Mark Jay Kushner

Director of Thesis Research

Timothy H. Field

Head of Department

Committee on Final Examination†

Chairperson

† Required for doctor's degree but not for master's.

MODELING THE REMOVAL OF SULFUR DIOXIDE AND NITROGEN OXIDES
FROM FLUE GASES USING COMBINED PLASMA AND OPTICAL PROCESSING

BY

JEANNE HICKMAN BALBACH

B.A., University of Illinois, 1970

THESIS

Submitted in partial fulfillment of the requirements
for the degree of Master of Science in Electrical Engineering
in the Graduate College of the
University of Illinois at Urbana-Champaign, 1991

Urbana, Illinois

ABSTRACT

Combined plasma photolysis (CPP) is a process that uses a pulsed electrical discharge in flue gases (Air/H₂O/SO₂/NO_x) followed by irradiation with ultraviolet photons to cause simultaneous removal of SO₂ and NO_x from the gas stream. Combined plasma photolysis causes the efficient production of hydroxyl radicals which react with SO₂ and NO_x to produce sulfuric acid and nitric acid, respectively. These acids are easily removable from the gas stream. A computer model including a self-consistent accounting of the electron impact, plasma chemistry and radiation transport for a pulsed gas discharge illuminated by ultraviolet photons has been developed to simulate the CPP process. The results of this model are verified by comparison with experimental data. Various gas mixtures, light intensities and energy depositions are examined.

ACKNOWLEDGEMENTS

I would like to thank Professor Mark Jay Kushner for his guidance and direction and, in particular, his willingness to further my education at all opportunities. Professor Mark Rood and his assistant Moo Been Chang were most helpful in providing the experimental complement to this project. Tom Keating, Mike Hartig, Rich Fraser, Yilin Weng, Hoyoung Pak and Ann Farkas kept my enthusiasm at a high level and encouraged me to remember that there is a world outside of my own. A special thanks to Mike McCaughey for his constant motivation and his many thoughtful suggestions.

My friend, Don Lowry from the Illinois State Geological Survey, provided much encouragement along with the necessary information concerning the contents of Illinois fossil fuel.

My family has been wonderful. My parents Mal and Peg Hickman, my parents-in-law Stan and Sarah Balbach, and especially my husband Byron and my children John, James, Richard and Judith have my deepest appreciation. I know that they have been through several stressful years having a daughter, wife or mother "still in school." My family has been greatly supportive and a source of constant encouragement.

My sincere thanks to you all.

TABLE OF CONTENTS

	Page
1. INTRODUCTION	1
1.1 Background	1
1.2 Combined Plasma Photolysis (CPP)	1
2. DESCRIPTION OF THE MODEL	7
2.1 Overview	7
2.2 Description of the Model	7
2.2.1 The circuit model	8
2.2.2 Calculation of the electron impact rate coefficients	9
2.2.3 Plasma chemistry and photo-physics models	11
3. RESULTS	14
3.1 Use of the Computer Model	14
3.2 Experimental Verification	14
3.3 Primary Reaction Pathways	18
3.4 Energy Deposition	22
3.5 Optical Processing	24
3.6 Gas Temperature	28
3.7 Gas Mixtures	29
3.8 Generation and Removal of Nitrogen Oxides	31
4. CONCLUSIONS	47
APPENDIX. SPECIES AND REACTIONS	49
REFERENCES	65

1. INTRODUCTION

1.1 Background

There is an increasing international demand to reduce the amount of SO_2 and NO_x emitted into the atmosphere by industrial and power plants burning fossil fuel. Combined Plasma Photolysis (CPP) is proposed as a gas phase removal process which will simultaneously remove SO_2 and NO_x from flue gases before the gas stream is released into the atmosphere[1],[2]. It is not the purpose of this thesis to examine the political or environmental issues surrounding the removal of SO_2 and NO_x from flue gas streams[3] or to analyze current removal systems¹. A computer model has been developed to simulate the CPP process. This model is validated with data obtained from an experimental setup of the CPP process. Using the model, removal results can be determined for a given set of initial conditions. The model will also be useful in determining proper levels of light and energy in order to achieve optimum removal conditions for differing gas mixtures.

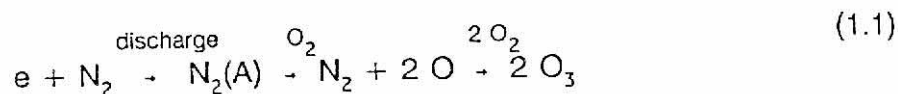
1.2 Combined Plasma Photolysis (CPP)

Combined plasma photolysis is the use of combined plasma and optical processing of flue gases. Air enters the boiler chamber (see Figure 1.1) where SO_2 ,

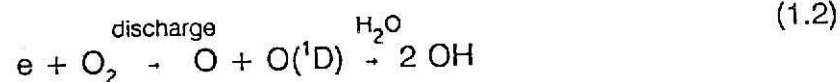
¹ Currently implemented systems include dry lime injection-electrostatic precipitator-selective catalytic reduction (SCR) systems, low NO_x burner-spray dryer-fabric filter systems, and electron beam-fabric filter systems.

NO_x , CO_2 and particulate material are added to the gas stream as fossil fuel is burned [4],[5],[6],[7]. (All figures appear at end of chapter.) Pretreatment of the flue gas may occur before it enters the reaction chamber. This pretreatment can consist of the addition of water, which results in humidification and evaporative cooling, and the addition of other substances such as ammonia (NH_3), which enhances the removal of the unwanted products of the combustion. Plasma oxidation of the flue gas occurs in the reaction chamber and is initiated by energetic electrons². These energetic electrons excite, ionize and dissociate the molecules in the flue gas, producing oxidants such as hydroxyl (OH), oxygen (O), and hydroperoxyl (HO_2) radicals. These radicals react with the SO_2 and NO_x , eventually producing sulfuric acid (H_2SO_4) and nitric acid (HNO_3). These acids may be easily removed from the gas stream.

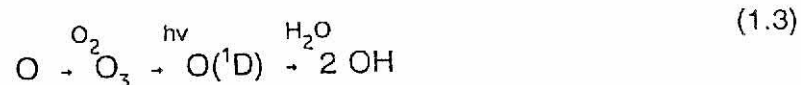
The efficient production of the hydroxyl radical is essential to the CPP process, which produces the hydroxyl radical through the creation of excited states and excitation transfer reactions in the gas. Two excitation reactions are of importance:



² Methods of producing these energetic electrons include electron-beam, dc discharge, pulsed streamer corona discharge, high frequency discharge or transversely excited atmospheric discharges.



Production of the hydroxyl radical can be further increased by the use of ultra-violet photons ($\lambda \leq 325$ nm), which produce $O(^1D)$ by the photon dissociation of ozone which is one of the by-products of the plasma processing:



The hydroxyl radical is an essential reactant in the formation of sulfuric and nitric acids. The optimum rate of removal can be calculated from the excitation rate and the acid-formation reactions. Two hydroxyl radicals are required to convert one SO_2 molecule to sulfuric acid.



The highest removal rate for CPP processing is

$$\frac{d[SO_2]}{dt} = -2.0 (\text{Excitation Rate}) \quad (1.5)$$

The conversion of one molecule of NO to nitric acid requires three hydroxyl radicals.



The highest removal rate for CPP processing is

$$\frac{d[\text{NO}]}{dt} = -1.33 \text{ (Excitation Rate)} \quad (1.7)$$

Considering NO_2 , another oxide of nitrogen which occurs in large concentrations in flue gases, only one OH radical is required for conversion to nitric acid.



For CPP processing, the highest removal rate is

$$\frac{d[\text{NO}_2]}{dt} = -4.0 \text{ (Excitation Rate)} \quad (1.9)$$

Removal efficiency is defined as the amount of SO_2 or NO_x removed (in parts per million) divided by the energy deposited in the gas. One of the primary products from excited states in atmospheric gases is ozone. Only a fraction of these excited states result in the production of the hydroxyl radical [8]. Ozone as a terminal product does not contribute to removal of SO_2 or NO_x from the gas. Thus a major portion of the deposited energy in plasma processing is wasted. Combined plasma photolysis utilizes the ozone through optical processing and continues the creation of the excited oxygen atoms, thereby enhancing the generation of the hydroxyl radical after direct plasma processing has terminated.

The removal efficiency as a function of the energy deposited can be determined by comparing the energy required for production of the necessary excited states by plasma excitation and photolysis. For SO_2 removal efficiency:

$$\frac{\Delta[\text{SO}_2]}{[\text{SO}_2]} = - \frac{25 \cdot E_{\text{DEP}} (\text{mJ} \cdot \text{cm}^{-3})}{[\text{SO}_2] \text{ ppm}} \quad (1.10)$$

Combined plasma photolysis processing of NO results in the following removal efficiency:

$$\frac{\Delta[\text{NO}]}{[\text{NO}]} = - \frac{16 \cdot E_{\text{DEP}} (\text{mJ} \cdot \text{cm}^{-3})}{[\text{NO}] \text{ ppm}} \quad (1.11)$$

The removal efficiency for processing of NO_2 is

$$\frac{\Delta[\text{NO}_2]}{[\text{NO}_2]} = - \frac{50 \cdot E_{\text{DEP}} (\text{mJ} \cdot \text{cm}^{-3})}{[\text{NO}_2] \text{ ppm}} \quad (1.12)$$

The keys to the CPP approach which should make it attractive are (1) the efficient generation of the necessary excited states by a low energy discharge and (2) the efficient photolysis of the ozone by commercially available UV lamps³.

³ The commercially available UV light sources are fluorescent lamps (Ar/Hg low pressure discharges) which produce a wavelength of 254 nm with 75% electrical efficiency. In fluorescent lamps for everyday use, this wavelength is absorbed by phosphorus in a coating on the glass and emitted as visible light. Thus the UV light sources are modified fluorescent lamps without the phosphor coating. High pressure Hg lamps may operate with high photon fluxes but lower efficiency.

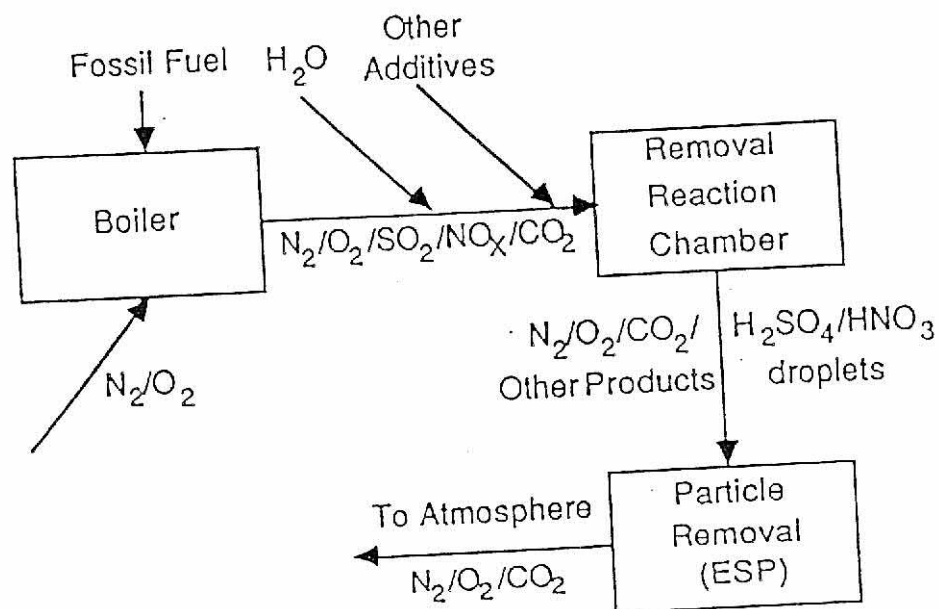


Figure 1.1 Schematic of the flue gas processing system including the boiler in which the fossil fuel is burned in the presence of air, the addition of water and other additives to the gas stream, the removal reaction chamber in which the CPP processing occurs, and finally the particle removal system.

2. DESCRIPTION OF THE MODEL

2.1 Overview

A computer model simulating the CPP process has been developed. This model includes a self-consistent accounting of the electron impact, plasma chemistry and radiation transport in a pulsed gas discharge being illuminated by ultraviolet photons. A literature search was performed to determine the important chemical reactions that occur in such a system. The Appendix contains a list of the species and reactions which are used in the model. Gas temperature-dependent reaction rates are used if available; otherwise, these reaction rates were generically scaled. Photolysis reactions for absorption of 254 nm light are included for each appropriate species in the model. Electron impact cross sections for the dominant chemical species in the model (N_2 , O_2 , CO_2 , H_2O) are used to determine reaction rates. The model is a zero-dimensional plug-flow simulation.

2.2 Description of the Model

The computer model used to simulate CPP consists of three main components (see Figure 2.1), each of which is described in detail in the following sections. The first circuit model determines an E/N value¹. This E/N value is used to solve Boltzmann's equation for the electron energy distribution which is then used to

¹ E/N is the amplitude of the electric field divided by the density of the gas. This E/N value usually is given in units of Townsends (Td) where $1 \text{ Td} = 10^{-17} \text{ V-cm}^2$.

compute the necessary electron impact rate coefficients. These rate coefficients are combined with the temperature-dependent rate coefficients and the densities of the various species to calculate the time derivatives of the plasma species. The photo-physics of the system may be included in these calculations. The conductivity of the plasma is computed and is used to calculate the resistance of the plasma for use in solving the circuit equations.

2.2.1 The circuit model

A schematic circuit representing that used in the computer model is shown in Figure 2.2. The storage capacitor is given an initial voltage. The switch is closed and the circuit equations are integrated for the flow of current through the system.

These equations are

$$\frac{d}{dt} I_{DIS} = (V_{HEAD} - V_{DIS} - R_{HEAD} \cdot I_{DIS}) \div L_{HEAD} \quad (2.1)$$

$$\frac{d}{dt} V_{HEAD} = (I_{LINE} - I_{DIS}) \div C_{HEAD} \quad (2.2)$$

$$\frac{d}{dt} I_{LINE} = (V_{LINE} - V_{HEAD}) \div L_{LINE} \quad (2.3)$$

$$\frac{d}{dt} V_{LINE} = I_{LINE} \div C_{LINE} \quad (2.4)$$

where

V_{DIS} is the voltage across the discharge,

I_{DIS} is the discharge current,

V_{HEAD} is the voltage across the peaking capacitor,

R_{HEAD} is the head resistance,

L_{HEAD} is the head inductance,

I_{LINE} is the line inductor current,

C_{HEAD} is the peaking capacitance,

V_{LINE} is the voltage across the storage capacitor,

L_{LINE} is the line inductance, and

C_{LINE} is the storage capacitance.

Before breakdown of the plasma occurs, there is no discharge current.

$$V_{\text{DIS}} = V_{\text{HEAD}} \quad (2.5)$$

As the circuit equations are integrated with time, the voltage across the plasma increases. Once a sufficiently high voltage is obtained, breakdown of the plasma occurs and electric current flows through the plasma.

$$V_{\text{DIS}} = I_{\text{DIS}} \cdot R_{\text{DIS}} \quad (2.6)$$

I_{DIS} is determined in part by the conductivity of the plasma. This conductivity depends on the plasma reactions that have occurred. The discharge voltage divided by the gas density determines the E/N value that is used in solving Boltzmann's equation.

2.2.2 Calculation of electron impact rate coefficients

The distribution of electron energies is obtained by solving Boltzmann's equation. This distribution is calculated for a specific gas mixture and a specific E/N which is determined in the circuit model. The electron distribution functions are non-

Maxwellian as is expected in molecular gas mixtures. A comparison of the electron energy distribution functions for four different E/N values for the same gas mixture is shown in Figure 2.3. For the smallest E/N (5 Td), the majority of electrons is of very low energy. Elastic momentum transfer is the dominant electron impact process. At this E/N, there is some small number of electrons with enough energy to engage in inelastic electron impact processes (vibrational, excitational or ionizational). As E/N is increased, a larger fraction of the electrons have higher energies. For the highest E/N (200 Td), a majority of the electrons have energies high enough so that excitational and ionizational processes frequently occur.

From the electron energy distribution function $f(\epsilon)$, a rate coefficient k is calculated.

$$k = \int f(\epsilon) \sigma(\epsilon) v(\epsilon) d\epsilon \quad (2.7)$$

where $\sigma(\epsilon)$ represents the electron impact cross section for the reaction process for which the rate coefficient is being calculated and $v(\epsilon)$ is electron velocity.

A thorough literature search was performed to compile electron impact cross sections of the major molecular species of the CPP model (N_2 , O_2 , H_2O , and CO_2). A total of fifty-seven cross sections are used to determine the electron energy distribution. A sequence of E/N values from 1 to 1000 Td is chosen and the electron energy distribution function calculated for each value. From the distribution functions a rate coefficient can be determined for each electron impact reaction. These rate coefficients are entered into a look-up table as a function of E/N. As the circuit

model computes an E/N , this value is used to determine the appropriate rate coefficient that is used for the electron impact reactions listed in the Appendix. If the E/N determined by the circuit model is not one of the exact values for which a rate has been calculated, an interpolation is performed to find the appropriate rate coefficient.

2.2.3 Plasma chemistry and photo-physics models

The electron impact rate coefficients are combined with the gas temperature-dependent rate coefficients and the densities of the various chemical species to form rate equations for the plasma chemistry. All reactions listed in the Appendix are available in the model although only a fraction of these will be used in a given calculation. A reaction will not be included in a calculation if any one of the reactants is missing. The photo-physics of the system is incorporated into the model at this stage through the use of rate coefficients developed from the optical cross sections at 254 nm.

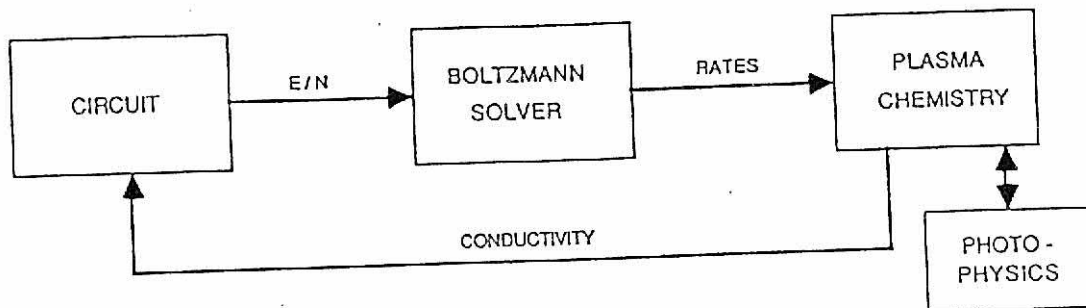


Figure 2.1 Schematic of the computer model with the three main sections being (1) the circuit model which determines an E/N value to be used in (2) the Boltzmann solver that computes the necessary electron impact rate coefficients to be used in (3) the plasma chemistry and appropriate photo-physics.

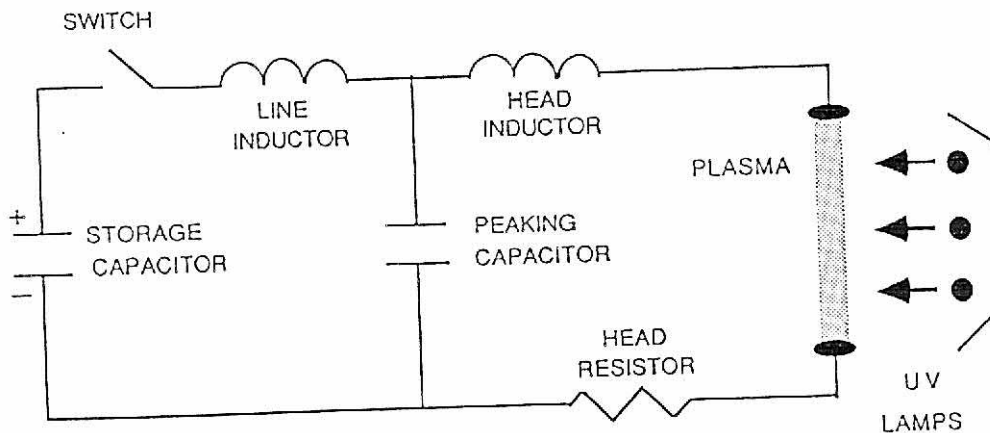


Figure 2.2 Schematic of the circuit used in the computer model.

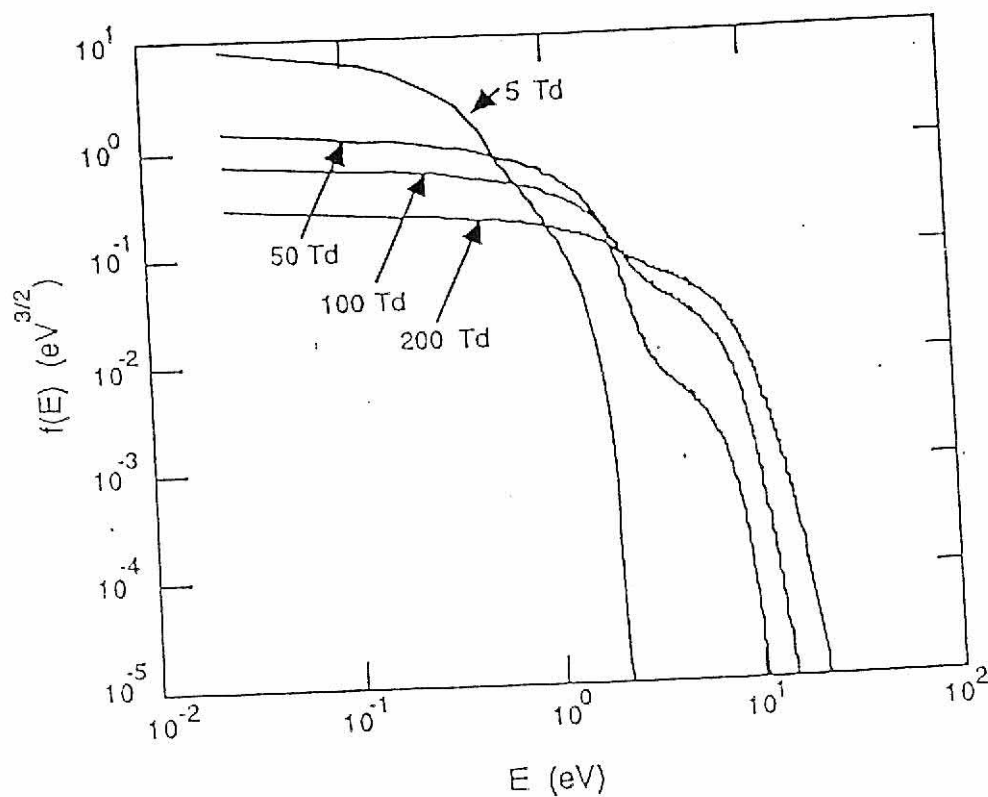


Figure 2.3 The electron energy distribution function at $E/N = 5, 50, 100$, and 200 Td for a gas mixture of $\text{N}_2/\text{O}_2/\text{H}_2\text{O} = 84/6/10$. The lowest E/N has the majority of the electrons distributed at very low energies. As the E/N increases, an increasing fraction of the electrons have higher energies.

3. RESULTS

3.1 Use of the Computer Model

The computer model has been validated by comparing computed results with experimental results. Such validation has demonstrated that the computer model contains all the essential elements to accurately simulate CPP. Computer simulations of CPP can be used to predict removal results given a set of initial conditions or to optimize removal results based on initial gas compositions. The primary reaction pathways of the major species can be examined in detail.

In modeling the CPP process, some initial parameters remain constant. Since this is an open system, a gas pressure of one atmosphere is always assumed. In most instances, the rate coefficients in the model are valid only in a temperature range of 240 °K to 600 °K; therefore, simulations are limited to this range. The parameters that can be varied are light intensity, gas mixture and energy deposition.

3.2 Experimental Verification

An experimental model of the CPP process has been constructed¹. The initial and final densities (in parts per million) of SO₂ are measured yielding a removal percentage. The by-products from CPP processing of SO₂ were not measured experimentally. The initial mixture, temperature, and pressure of the gas are

¹ The experimental work in the development of the CPP process is being done by Mark Rood and Moo Been Chang of the Department of Civil Engineering, University of Illinois at Urbana-Champaign.

measured for these experiments and are used as initial conditions in computer simulations. Since the total energy deposition is not accurately known for the experimental model, the computer model is normalized by varying the amount of energy deposition to obtain results comparable to experimental results.

In the experimental model, the initial density of SO_2 is varied and the fractional amount of SO_2 removed is measured for each case. The gas mixture in each case is $\text{N}_2/\text{O}_2/\text{H}_2\text{O} = 77/21/2$. The gas temperature is 300 °K. The computer model is normalized to the experimental model for an initial SO_2 density of 1000 ppm. The removal percentages of SO_2 as a function of the initial density of SO_2 are shown in Table 3.1. Results from computer simulations closely match the experimental results for initial SO_2 densities of 1000 and 2000 ppm. The computer simulation shows smaller fractional removal than is achieved experimentally when the initial density of SO_2 is reduced to 500 ppm.

Table 3.1 Fractional removal of SO_2 as a function of initial SO_2 density.

Initial SO_2 Density (parts per million)	Percent Removal Experimental Results	Percent Removal Computer Results
2000	22%	24%
1000	30%	30%
500	54%	42%

Cases are compared in which the residence time in the experimental reaction chamber is reduced from 5 seconds to 2.5 s. The initial SO_2 density is 1000 ppm in a gas mixture of $\text{N}_2/\text{O}_2/\text{H}_2\text{O} = 77/21/2$ at a gas temperature of 300 °K. The computer model is normalized for a residence time of 5 s by determining the even number of pulses needed to obtain the same fractional removal as is achieved with the experimental processing. A second simulation is made using half this number of pulses. This second simulation corresponds to a residence time of 2.5 s in the reaction chamber. The results are shown in Table 3.2. For a residence time of 2.5 s, a higher fractional removal is obtained for the computer simulation than is observed experimentally.

Table 3.2 Fractional removal of SO_2 as a function of time.

Time (seconds)	Percent Removal Experimental Results	Percent Removal Computer Results
5.0	30%	30%
2.5	12%	15%

A series of six experiments is performed in which the initial density of SO_2 is constant (1000 ppm) and the oxygen fraction of the gas mixture is varied (0, 3, 5, 10, 15 and 21%). The water fraction remains constant at 2%. The remainder of the gas

mixture is nitrogen. The gas temperature is 300 °K. A corresponding series of six simulations are computed. The computer model is normalized using an initial oxygen content of 21%. The resulting SO₂ fractions of removal for both the experimental and the computer models are shown in Figure 3.1. As the fractional amount of O₂ is increased, the fractional removal of SO₂ increases. Except for the case in which no oxygen is present, the computer results are very close to those for the experiment.

The experimental model has a plasma excitation rate of 120 Hz. The gas remains in the reaction chamber from 2.5 to 5 s. Thus, between 300 and 600 discharge pulses are used to process the gas. It is not feasible to simulate this number of pulses with the computer model. Six pulses or less can be simulated easily without using vast amounts of computational time. A comparison of the density of SO₂ using one, two, four, six and eight pulses is shown in Figure 3.2. In each case, the total energy deposited is 130 mJ·cm⁻³. The initial density of SO₂ (1000 ppm) is the same. The total removal of SO₂ increases as the number of pulses increases up to a maximum of six pulses. The energy deposited per pulse decreases as the number of pulses increases. Increasing the number of pulses beyond six yields a decrease in the fractional amount of SO₂ removal because the energy deposition per pulse is too small to achieve maximum removal. Since the energy deposition for the experimental model is not accurately known, the computer model can be normalized by an energy deposition which yields the same fractional removal as that obtained experimentally. A small number of pulses with maximum efficiency of removal need to be used for computer simulation. The computational

time required is approximately the same per pulse. A compromise between the amount of computational time used and the number of pulses needed for experimentally comparable results must be reached.

The comparison of the computed and experimental results from these three series verifies that the computer model contains all the essential elements to accurately simulate CPP in the case of SO_2 removal. These results also show that a close approximation of the actual results may be obtained from a computer simulation without using large amounts of computer resources to perform additional iterations.

3.3 Primary Reaction Pathways

Using the computer model, an analysis of the processes causing production and depletion of the important species contained in the model can be done. The major reaction pathways for OH, O_3 , SO_2 , NO and NO_2 are identified. This analysis can be used in determining the optimum conditions for removal of SO_2 and NO_x .

Combined plasma photolysis is based on the efficient production of the hydroxyl radical (OH) which is important in the formation of sulfuric and nitric acid from SO_2 and NO_x . The dominant reaction sequence in the production of this radical is shown in Figure 3.3. A typical trace of the OH density during and after a discharge pulse is shown in Figure 3.4. The initial high density peak of the hydroxyl radical in the region labeled I is formed by direct electron impact with water. Depletion of the radical density occurs by OH reacting primarily with SO generating

SO₂. A second peak in region II results from the reaction of H₂O with O(¹D). After the discharge pulse is over, depletion of the hydroxyl density in region III continues by reaction of OH with SO₂ and NO_x to form sulfuric acid and nitric acid. The depletion of the hydroxyl density can be slowed by formation of OH from H₂O reacting with O(¹D) created by photolysis of ozone. The efficiency of the hydroxyl radical production is decreased by (1) quenching of O(¹D) by a molecule other than H₂O, (2) interception of oxygen atoms before the formation of ozone, and (3) quenching of N₂(A) by molecules other than O₂. Cases two and three are of special concern if optical processing is to be used.

The photolysis of ozone will continue the generation of O(¹D) after the discharge pulse ends. Without photolysis, ozone is a fairly inert by-product of the plasma processing. Ozone is not the only species sensitive to 254 nm light in this model; however, ozone does have the largest optical absorption cross section². The reaction sequence producing ozone and some of the species with which ozone reacts is shown in Figure 3.5. It is apparent from examining a typical trace of the ozone density as shown in Figure 3.6 that ozone is primarily a terminal product unless photolysis occurs. The initial peak in density is produced by reaction of oxygen atoms with molecular oxygen. The ground state oxygen atom is formed by quenching of an excited oxygen atom or by the dissociation of molecular oxygen by reaction with N₂(A). The small fraction of the ozone that reacts with other species is

² These species and their optical cross sections at 254 nm are listed in the Appendix.

offset by a continued small production of ozone. If optical processing is not used, a steady-state ozone density is achieved. When photolysis is used, the ozone density is rapidly reduced and the desired $O(^1D)$ atom is produced.

The primary reaction sequence in the depletion and production of SO_2 is shown in Figure 3.7. Typical traces of the density of SO_2 during and after a discharge pulse are shown in Figure 3.8. In this example, SO_2 removal is shown for two standard gas mixtures. One mixture contains only N_2 , O_2 , and H_2O , while the second mixture adds CO_2 . Both mixtures have the same initial density of SO_2 (1000 ppm). The initial removal shown in region I occurs by direct reaction of SO_2 with $N_2(A)$ forming primarily the SO radical. The gas mixture containing CO_2 shows less initial removal. There is a smaller percentage of nitrogen in the mixture containing CO_2 , and less $N_2(A)$ is formed and used in the removal process. The SO radical quickly oxidizes to form primarily SO_2 . Other products of this oxidation such as HSO_3 react to form H_2SO_4 . A steady removal of SO_2 continues to occur in region III by reaction of SO_2 with OH and HO_2 radicals and with H_2O . Although many intermediate products can be formed, the terminal species in this sequence is H_2SO_4 .

With both nitrogen and oxygen having large mole fractions, the formation of NO_x occurs during plasma processing. Nitrogen oxides (NO_x) refer to NO, NO_2 , and NO_3 . Only NO and NO_2 are formed in appreciable quantities. The primary production sequence for NO_x is shown in Figure 3.9. Nitric oxide (NO) is formed from either excited or ground state atomic nitrogen reacting with oxygen in its atomic or molecular state, ozone or the hydroxyl radical (HO_2). Although NO is quickly

formed, it rapidly reacts with a number of species to form NO_2 . There is some conversion of NO_2 back to NO but this process proceeds at a smaller rate compared to the forward reactions. Regardless of whether optical processing is used, a peak in the density of NO is quickly formed. From this peak value, the density of NO decreases. Two typical traces of NO density during and after a discharge pulse are shown in Figure 3.10. The decrease in the density of NO is much more rapid in the case in which illumination is used.

Once the NO_2 molecule is formed, a number of conversion and reformation sequences occur (see Figure 3.11). There is some conversion of NO_2 to NO but the formation of NO_2 from NO is the dominant process. The nitrate radical (NO_3) is formed from NO_2 . It also reacts with several species including itself to form NO_2 or to form other intermediate species which primarily convert to NO_2 , which will ultimately form nitric acid (HNO_3) by reacting with OH . However, this acid is sensitive to illumination at 254 nm, which is the wavelength used in CPP, and dissociates to produce NO_2 . Fortunately, the optical absorption cross section for HNO_3 at 254 nm is fairly small ($1.9 \times 10^{-20} \text{ cm}^2$). The density of NO_2 with and without optical processing is shown in Figure 3.12. Using illumination, NO forms NO_2 rapidly and a steady-state is reached. Without using illumination, a steady-state density level takes longer to achieve and is ultimately at a higher value than with the use of illumination.

3.4 Energy Deposition

The manner and amount of the energy deposition have a large effect on the total amount of SO_2 removed and also on the efficiency of removal (amount removed per energy deposited per volume). Density traces of SO_2 are shown in Figure 3.13 for four values of energy deposition. The plasma excitation rate is 120 Hz. As the energy deposition per pulse is increased, the total removal increases. The fractional removal for the smallest energy deposition per pulse ($17 \text{ mJ}\cdot\text{cm}^{-3}/\text{pulse}$) is 24.7%. This fractional removal increases to 31.4% for an energy deposition of $22 \text{ mJ}\cdot\text{cm}^{-3}/\text{pulse}$. For an energy deposition of $27 \text{ mJ}\cdot\text{cm}^{-3}/\text{pulse}$, the fractional removal is 38.9%. This fractional removal increases to 44.8% for the largest energy deposition shown ($33 \text{ mJ}\cdot\text{cm}^{-3}/\text{pulse}$). This trend occurs under all sets of initial conditions studied. A greater amount of energy deposition yields a larger fractional amount of SO_2 removal.

The efficiency of removal of the CPP process is examined in two ways. The SO_2 efficiency of removal is the amount of SO_2 removed per energy deposited per volume of gas. The total efficiency of removal is the amount of SO_2 removed combined with the amount of production or removal of other species per unit of energy deposited per volume of gas. The other species considered in this efficiency are NO , NO_2 , NO_3 , SO , and SO_3 . If SO_2 is removed and any of these species are produced, the elimination of unwanted species from the gas stream has not occurred.

Both the SO_2 efficiency of removal and the total efficiency of removal do not continue to increase as more energy is deposited. For this series of cases, the removal efficiencies increase slowly and a maximum is reached at $27 \text{ mJ-cm}^{-3}/\text{pulse}$. The SO_2 removal efficiency is $3640 \text{ ppb/mJ-cm}^{-3}$ while the total removal efficiency is $3480 \text{ ppb/mJ-cm}^{-3}$. (The units of ppb are parts per billion.) Increasing the deposition to $33 \text{ mJ-cm}^{-3}/\text{pulse}$ decreases the SO_2 removal efficiency to $3410 \text{ ppb/mJ-cm}^{-3}$ and the total removal efficiency to $3250 \text{ ppb/mJ-cm}^{-3}$. By increasing the amount of energy deposited per pulse, more SO_2 is actually removed from the gas but the efficiency of this removal reaches a maximum and then decreases rapidly.

Another comparison of energy deposition is shown in Figure 3.14. Two amounts of total energy deposition (60 mJ-cm^{-3} and 100 mJ-cm^{-3}) are shown. For each amount of total energy, two types of deposition are considered: (1) total energy deposited in one pulse and (2) energy deposited in four pulses. The first pulse in each case demonstrates again that the larger the amount of energy deposition, the greater the fractional amount of SO_2 removal. For each total amount of energy deposition, more SO_2 removal occurs for the four-pulse example than for the one-pulse case. The percentage of SO_2 removal for the 60 mJ-cm^{-3} cases increases slightly from 19.3% for one-pulse deposition to 20.1% for a four-pulse deposition. Increasing the total energy deposition to 100 mJ-cm^{-3} yields a percentage of SO_2 removal of 25.6% for deposition in one pulse which increases to 36.4% for deposition in four pulses. Depositing the energy in four pulses as opposed to one pulse yields

an increase of 4% for the $60 \text{ mJ}\cdot\text{cm}^{-3}$ cases and an increase of 30% SO_2 removal for the $100 \text{ mJ}\cdot\text{cm}^{-3}$ cases. The fractional removal of SO_2 for a given energy deposition increases if the energy is deposited in a number of small pulses rather than one high energy pulse.

The efficiency of removal also increases if the energy is deposited in a series of small pulses rather than one high energy deposition. The initial conditions (gas mixture, temperature, and SO_2 density) are the same in these cases as for the cases used to show the effects of an increased energy deposition per pulse. The case of $100 \text{ mJ}\cdot\text{cm}^{-3}$ deposited in four pulses is near the maximum removal efficiency for the conditions used. Thus, the 30% increase in the SO_2 removal is close to the maximum value. If larger amounts of total energy are used, both the increase in the SO_2 fractional removal and the efficiency of SO_2 removal will gradually decline.

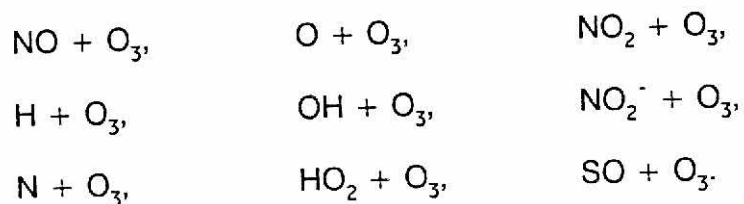
3.5 Optical Processing

Using optical processing in addition to plasma processing is the unique feature of CPP. The continued production of the hydroxyl radical from the $\text{O}(^1\text{D})$ atom generated by photolysis of ozone enhances the removal of SO_2 and NO_x . The effects of optical processing are examined in several ways with the computer model. A comparison is made between the dark case (plasma processing only) and the light case (plasma and optical processing). The intensity of the light can be varied. The time period of illumination is also studied.

The densities of SO_2 , NO and NO_2 as a function of time under five different light intensities during and after the first pulse of a 120 Hz excitation are shown in Figures 3.15 through 3.17. The energy deposition is the same in all cases; therefore, the effect of the plasma processing is the same. Thus the effects of optical processing can be differentiated. Even with a minimum intensity of light ($5 \text{ W}\cdot\text{cm}^{-2}$), the fractional removal of SO_2 is increased over the dark case. This increase is from 8.7% for the dark case to 12.1% using an intensity of $5 \text{ W}\cdot\text{cm}^{-2}$. The fractional removal of SO_2 reaches a maximum of 16.5% using an intensity of $50 \text{ W}\cdot\text{cm}^{-2}$. Increasing the intensity of the light to an amount greater than $50 \text{ W}\cdot\text{cm}^{-2}$ does not yield a greater fractional removal of SO_2 . Since the energy deposition is the same in all cases, the SO_2 removal efficiency also reaches a maximum at $50 \text{ W}\cdot\text{cm}^{-2}$ and does not change by increasing the light intensity. The density of NO reaches a peak and slowly decreases in the dark case, but reaches this same maximum value and decreases more rapidly with increasing intensity of light. With a 120 Hz excitation rate, the maximum decrease in the density of NO is obtained again using an intensity of $50 \text{ W}\cdot\text{cm}^{-2}$. Increasing the intensity of light does not yield a further decrease in the density of NO . The production of NO_2 reaches a steady-state level with illumination whereas production continues unimpeded in the dark case. The steady-state density level of NO_2 is smallest when using an intensity of $50 \text{ W}\cdot\text{cm}^{-2}$. Increasing the intensity of light above $50 \text{ W}\cdot\text{cm}^{-2}$ increases the dissociation of HNO_3 , N_2O_5 and HO_2NO_2 by light. Nitrogen dioxide (NO_2) is a product of these dissociations. The total efficiency for an initial SO_2 concentration of 1000 ppm reaches a

maximum using an intensity of 50 W-cm^{-2} . Increasing the intensity of light to 100 W-cm^{-2} decreases the total efficiency. The total efficiency continues to decrease as the intensity of light increases due to the increased dissociation of HNO_3 , N_2O_5 and HO_2NO_2 .

Calculation can be made of the minimum light intensity necessary so that the primary use of the photons will be dissociation of ozone into O_2 and $\text{O}(^1\text{D})$. To calculate the minimum amount of UV light that is necessary, a generic case is considered. A maximum density is assumed for ozone. A maximum density of each species for all reactions in which ozone is a reactant is determined. These reactions are



The maximum density of each species multiplied by the rate constant of that reaction generates an effective rate for each reaction. A total effective rate is the sum of the effective rates of the indicated reactions. The photolysis reaction is $h\nu + \text{O}_3$. Using again the maximum ozone density and the absorption rate coefficient for ozone, the rate of photolysis is calculated. Equating the total effective rate with the rate of photolysis and solving for $h\nu$ give an intensity of 20 W-cm^{-2} . At this intensity, the dissociation of ozone to $\text{O}(^1\text{D})$ and O_2 by ultraviolet photons will equal the consumption of ozone in other processes. Calculations for several specific cases were performed. In all cases, the minimum light intensity needed is approximately 20

$\text{W}\cdot\text{cm}^{-2}$. For the dissociation process to be effective, this intensity must be exceeded. An intensity of $50 \text{ W}\cdot\text{cm}^{-2}$ obtains the maximum efficiency, and further increases in the intensity do not yield increased fractional removal but do yield a decrease in the total efficiency of removal.

The length of time in which light is used during and after a discharge pulse affects the fractional removal of SO_2 and also the efficiency of removal. The densities of O_3 and SO_2 during and after the first pulse of a 120 Hz excitation are shown in Figure 3.18. In all cases the intensity of light is $50 \text{ W}\cdot\text{cm}^{-2}$. The time periods of illumination are 1, 3, 5, and 7 ms. These time periods are compared to those for the dark case. After the discharge pulse, the density of O_3 is at a steady-state level unless there is illumination. Once the light is removed, the density of O_3 remains at essentially the same level. After plasma processing is completed, SO_2 is removed only with illumination. The removal of SO_2 ceases once the light is removed. A light period of more than 5 ms does not appreciably increase the fractional removal of SO_2 . The SO_2 removal efficiency also increases proportionally to the fractional removal increase. The same amount of energy for plasma processing is used in each case. Again, a time period of more than 5 ms does not appreciably increase the SO_2 removal efficiency. The total efficiency continues to increase by increasing the time of light use. The use of light reduces the amount of other unwanted species produced, and this reduction continues as long as there is illumination. Therefore, if only the removal of SO_2 is considered, the light can be pulsed. For maximum total removal efficiency, the light source needs to be on continuously.

3.6 Gas Temperature

Gas temperature dependences of reaction rates for the plasma chemistry for the range 240 to 600 °K are included in the reaction scheme (see the Appendix). If the temperature dependence of a specific reaction is not known, a "generic" dependence is used. For two-body reactions the dependence is $[T_{\text{gas}}/300]^{0.5}$ to reflect the increase in collision frequency. For three-body reactions, dependence is $[T_{\text{gas}}/300]^{-1.5}$. The dependence for ion-ion recombination is $[T_{\text{gas}}/300]^{-0.5}$. For electron-ion recombination, the dependence on electron temperature is $T_e^{-0.5}$.

The effect of initial gas temperature on the CPP process is shown in Figure 3.19. In both cases, the initial SO₂ density is 1000 ppm and the gas mixture is N₂/O₂/H₂O = 84/6/10. The initial gas temperatures are 410 °K and 500 °K. Densities are normalized to take into account the change in initial density with temperature. The fractional removal of SO₂ with an initial gas temperature of 410 °K is 61.5%. When the initial gas temperature is increased to 500 °K, the fractional removal of SO₂ increases to 69.5%. The efficiency of removal is also increased by increasing the initial gas temperature. The SO₂ efficiency is increased by 14.7%. The total efficiency of removal increases by 17.0%. This increased SO₂ removal results from changes in reaction rate coefficients involving the hydroxyl radical. As the gas temperature increases, the rate coefficients of reactions in the removal sequence involving the OH radical and the SO₂ molecule increase and become more important. Thus the removal of SO₂ is greater and more efficient at higher gas temperatures.

3.7 Gas Mixtures

The effect of the gas mixture on removal is examined by varying the fractions of H_2O , CO_2 and O_2 in the mixture. When varying H_2O from a mole fraction of 0.05 to 0.15, a very slight increase in the fractional removal of SO_2 for an initial density of 1000 ppm from 10.5% to 10.8% is obtained ($\text{N}_2/\text{O}_2/\text{H}_2\text{O} = 88.7/6.3/5.0; = 84/6/10.0; = 79.3/5.7/15.0$). The SO_2 removal efficiency and the total removal efficiency both reach a maximum at a mole fraction of H_2O of 0.10. In the case in which the mole fraction of H_2O is 0.05, not enough H_2O is present in the gas mixture to create the maximum amount of OH radicals necessary for the amount of energy deposited in the gas. In the case of a mole fraction of H_2O of 0.15, not enough O_2 is present in the gas mixture to effectively use the additional amount of H_2O . A balance between the amount of O_2 and H_2O present in the gas mixture must be maintained for efficient removal.

Upon adding CO_2 to the gas mixture and varying the mole fraction of water from 0.10 to 0.20, the fractional removal of SO_2 for an initial SO_2 density of 1000 ppm increases from 8.7% to 15.4% ($\text{N}_2/\text{O}_2/\text{H}_2\text{O}/\text{CO}_2 = 72.0/6.0/10.0/12.0; = 68.0/5.7/15.0/11.3; = 64.0/5.3/20.0/10.7$). The removal of SO_2 during and after the first pulse of a 120 Hz excitation is shown in Figure 3.20. The removal efficiencies do not continue to increase with an increasing mole fraction of H_2O . The SO_2 removal efficiency and the total efficiency are the greatest with a mole fraction of H_2O of 0.15. These efficiencies decrease by 26.4% and 28.1%, respectively, when the mole fraction of H_2O is increased to 0.20. These efficiencies show less decline (25.5% and 25.1%)

when decreasing the mole fraction of H_2O from 0.15 to 0.10. With a H_2O mole fraction of 0.10, there is not enough water in the mixture to generate the amount of OH radicals necessary for maximum efficient removal of the SO_2 and NO_x and conversion to H_2SO_4 and HNO_3 , respectively. In the case of a mole fraction of 0.20, enough water is present but the amount of O_2 in the gas mixture becomes the limiting factor. The mole fraction of water necessary for maximum efficiency of removal is greater with CO_2 in the gas mixture.

The addition of CO_2 to the gas mixture decreases the fractional removal of SO_2 but inhibits the generation of NO_x . The density of SO_2 as a function of time during the first millisecond of the first pulse of a 120 Hz excitation in two different gas mixtures, one containing CO_2 , is shown in Figure 3.21. The initial density of SO_2 in each mixture is 1000 ppm. More SO_2 is removed during the plasma processing phase without CO_2 in the gas mixture. One of the primary SO_2 removal reactions is the formation of SO from reaction with $\text{N}_2(\text{A})$. With a larger fraction of N_2 in the gas mixture, more $\text{N}_2(\text{A})$ is produced and available for reaction. The fractional removal of SO_2 is 10.7% which decreases to 8.7% upon adding CO_2 to the gas mixture. The addition of CO_2 decreases the fractional removal by almost 19%. However, the total efficiency decreases by only 13%. With the addition of CO_2 to the gas mixture, less NO_x is generated (380 ppb/mJ-cm⁻³ for the case with CO_2 compared to 290 ppb/mJ-cm⁻³ with CO_2 added to the gas mixture). This decrease in the amount of NO_x produced is due in part to the smaller fraction of N_2 present in the gas mixture. It is caused also by carbon compounds reacting with the precursors of NO_x .

The importance of oxygen in the removal process is shown by increasing the O_2 fraction of the gas mixture from 0% to 21%. The fractional removal of SO_2 increases from 1.8% to 20%. The water fraction remains constant at 2% in all cases. The density of SO_2 as a function of time and mole fraction of O_2 in the gas mixture during the first 100 μs of the first discharge pulse is shown in Figure 3.22. As the mole fraction of O_2 is increased, the amount of NO_x generated also increases from less than 1 ppb/mJ-cm⁻³ to 260 ppb/mJ-cm⁻³. There are two maximums in the efficiencies of removal. The first occurs when the fraction of O_2 is 3% of the gas mixture. The second maximum occurs with a mole fraction of 0.10. The first maximum occurs because a large fraction of the SO_2 is removed by reaction with $N_2(A)$. However, there is such a small amount of oxygen in the gas mixture that almost no NO_x is produced (20 ppb/mJ-cm⁻³). The efficiency decreases after the second maximum at a mole fraction of 0.10 because of a lack of water in the gas mixture; thus, an insufficient amount of OH radicals is generated in order to achieve maximum removal efficiency. For maximum effect, a balance between the amount of oxygen and water must be maintained. Both water and oxygen are necessary for the efficient removal of SO_2 and NO_x .

3.7 Generation and Removal of Nitrogen Oxides

The conditions of CPP processing affect the generation of NO_x . The addition of CO_2 to a gas mixture of $N_2/O_2/H_2O$ inhibits the production of NO_x . Increasing the mole fraction of O_2 in the gas mixture increases the amount of NO_x which is

generated. Optical processing inhibits the generation of and partially removes NO_x from the gas mixture. The greater the energy deposition during plasma processing, the greater the production of NO_x . Increasing the gas temperature decreases the production of NO_x .

If NO_x is initially present in the gas mixture, the fractional removal of SO_2 is greatly reduced. This is shown in Figure 3.23. For an initial SO_2 density of 1000 ppm, the fractional removal of SO_2 without an initial density of NO_x is 34.5%. This fractional removal reduces to 11.1% if an initial density of 1000 ppm of NO_x is present. The SO_2 removal efficiency likewise reduces. The case in which no initial NO_x is present has a generation of NO_x of $940 \text{ ppb/mJ-cm}^{-3}$, while the case in which 1000 ppm of NO_x is initially present has a total NO_x reduction of $1470 \text{ ppb/mJ-cm}^{-3}$. Thus, although the SO_2 removal efficiency decreases by 68% having an initial density of 1000 ppm of NO_x , the total removal efficiency only decreases by 28%. The densities of NO and NO_2 are shown in Figure 3.24. If initial densities of 500 ppm of NO and 500 ppm of NO_2 are present when CPP processing starts, the density of NO increases slightly while the density of NO_2 gradually reduces. Conditions such as the addition of optical processing can be established so that both the densities of NO and NO_2 are reduced. While the fractional removal of SO_2 is decreased by the addition of an initial concentration of NO_x , the total removal efficiency can be increased by using the removal conditions that inhibit the generation and enhance the removal of all species of NO_x .

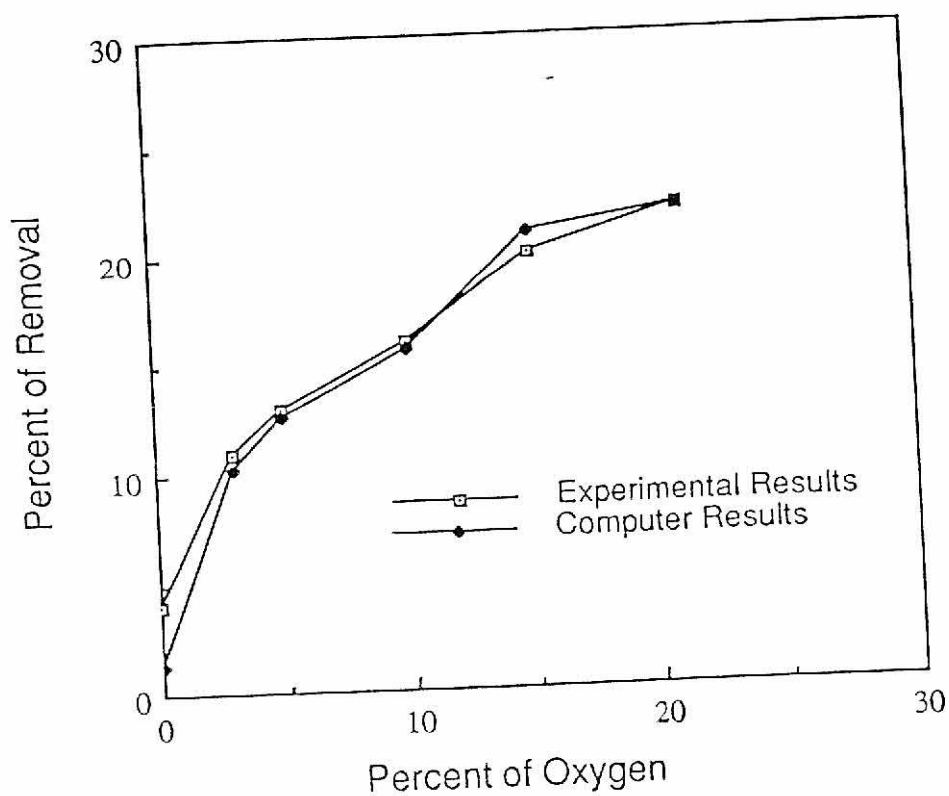


Figure 3.1 The fractional amount of SO_2 removal (initial density is 1000 ppm). The fractional amount of oxygen in the gas mixture is varied. Experimental results and computer results are plotted. As the fractional amount of oxygen in the gas mixture is increased, the fractional removal of SO_2 increases.

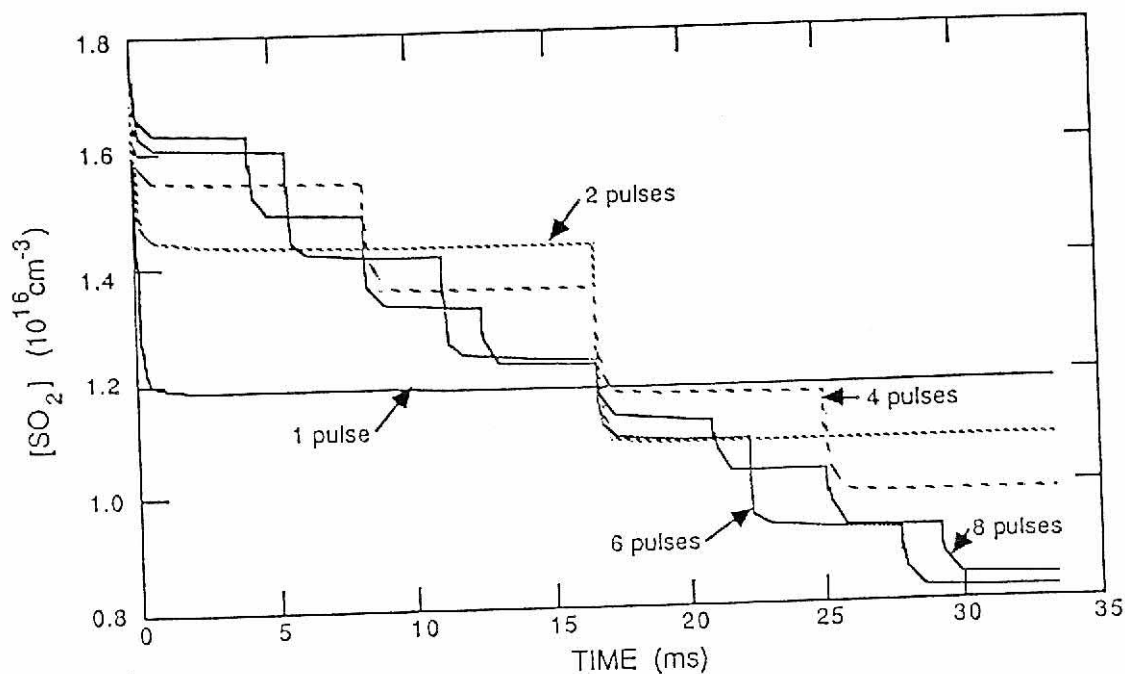


Figure 3.2 Traces of SO_2 density during series of discharge pulses. The initial density of SO_2 is 1000 ppm in a gas mixture $\text{N}_2/\text{O}_2/\text{H}_2\text{O} = 84/6/10$. The total energy deposited in every case is $130 \text{ mJ}\cdot\text{cm}^{-3}$. The number of pulses is one, two, four, six and eight.

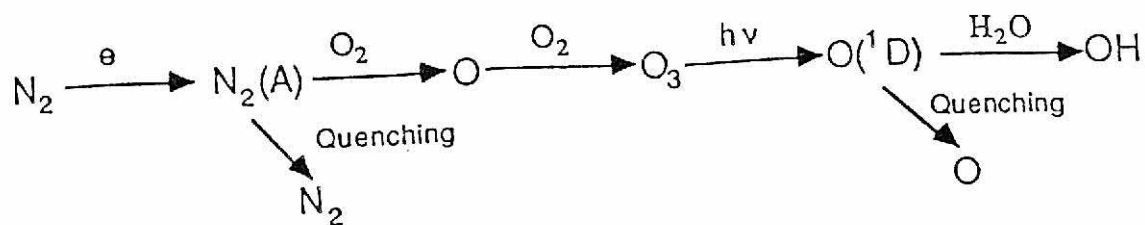


Figure 3.3 The primary reaction pathway in the production of the OH radical.

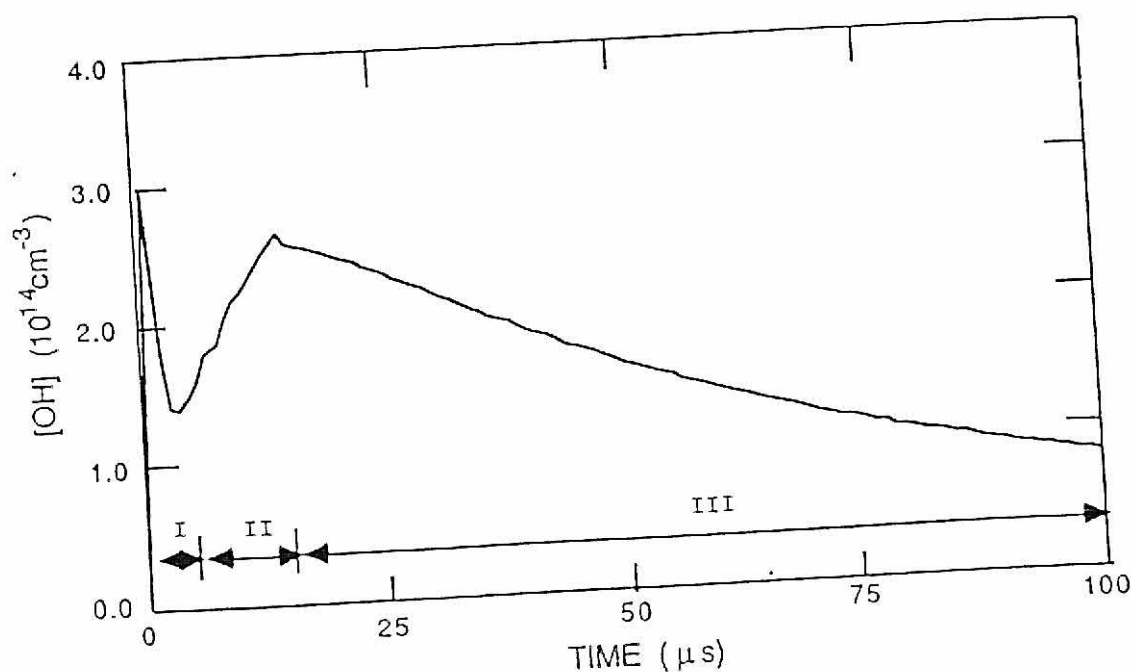


Figure 3.4 The density of OH during and after a discharge pulse. The initial density of the SO_2 is 1000 ppm. The gas mixture is $\text{N}_2/\text{O}_2/\text{H}_2\text{O} = 84/6/10$. Light intensity is 500 W/cm^2 . The initial density peak in Region I results from direct electron impact with H_2O . Depletion of the radical occurs primarily from oxidation of SO . In Region II further production occurs from reaction of H_2O with $\text{O}({}^1\text{D})$. Two competing processes are in Region III. Production of the OH radical occurs from the reaction of H_2O with $\text{O}({}^1\text{D})$ created from photolysis of ozone. The depletion of this radical is by reaction with any number of species in the plasma, preferably SO_2 and NO_x .

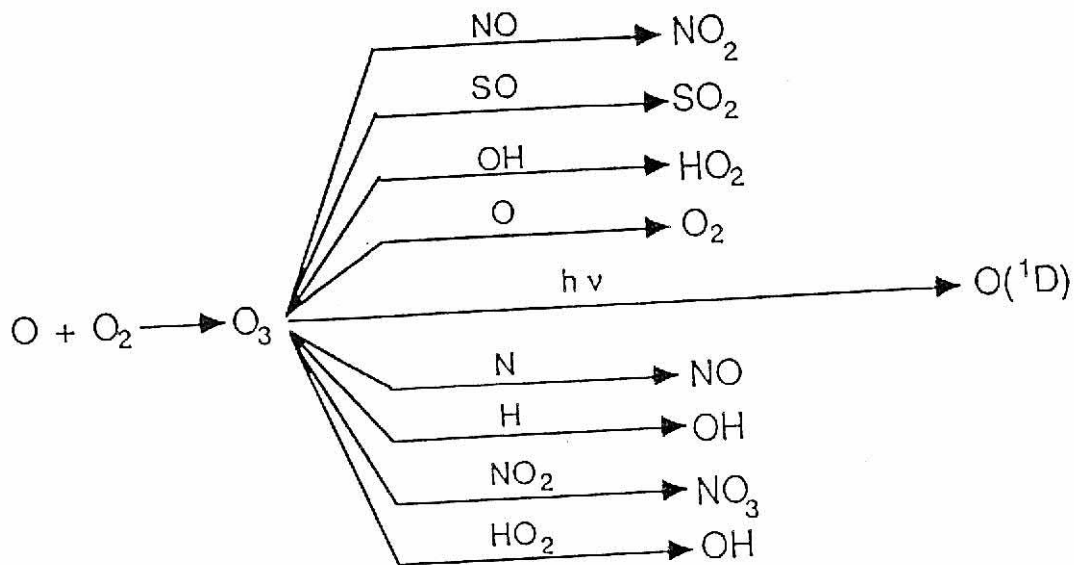


Figure 3.5 The primary reactions involving ozone. The only reaction rate of any magnitude involving ozone as a source term is $O_3 + h\nu$ forming $O(^1D)$. The other reaction rates are small in comparison.

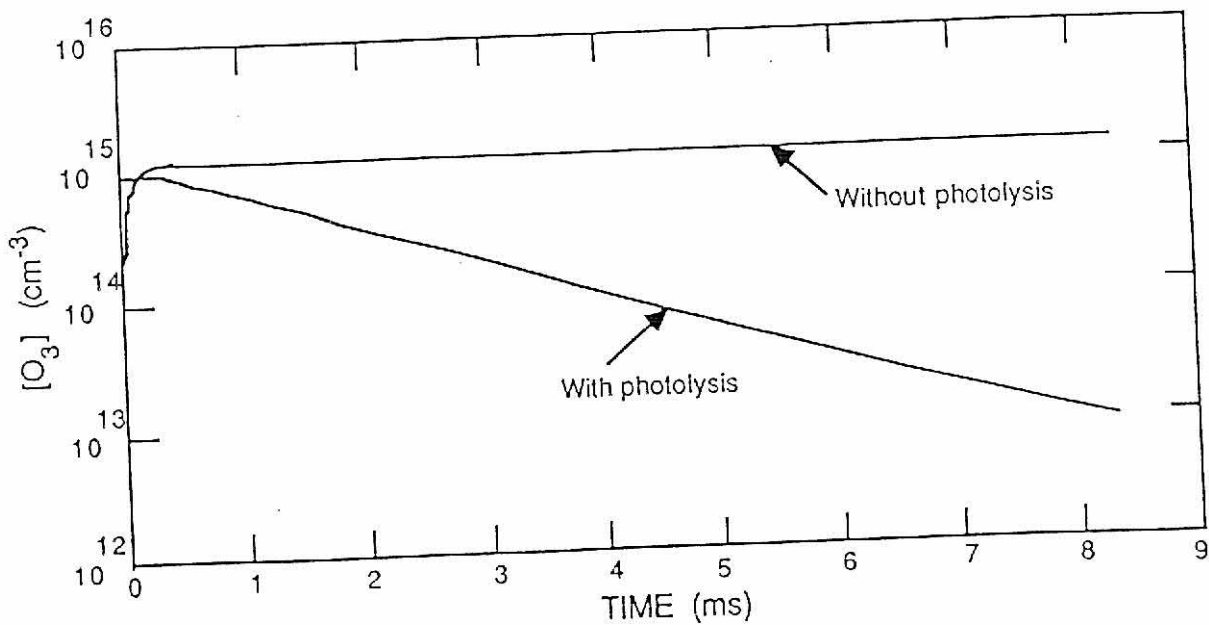


Figure 3.6 The density of O_3 during and after a discharge pulse in $N_2/O_2/H_2O/CO_2 = 72/6/10/12$ with and without illumination. With illumination, the intensity of the light is 50 W-cm^{-2} . Ozone is a terminal species unless photolysis is used.

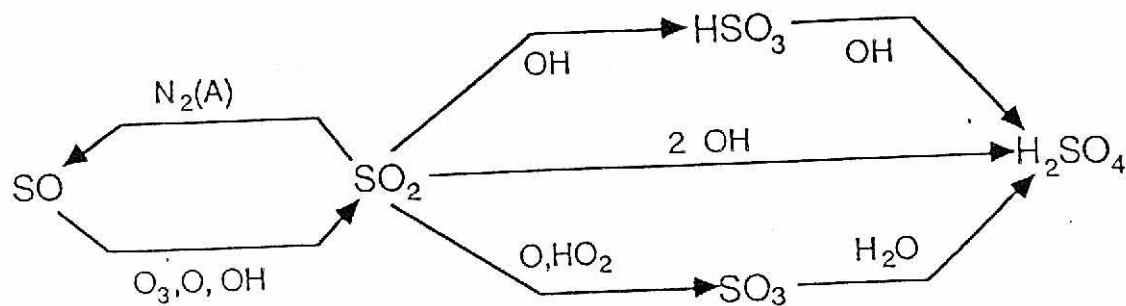


Figure 3.7 The primary reaction sequences in the depletion and production of SO_2 .

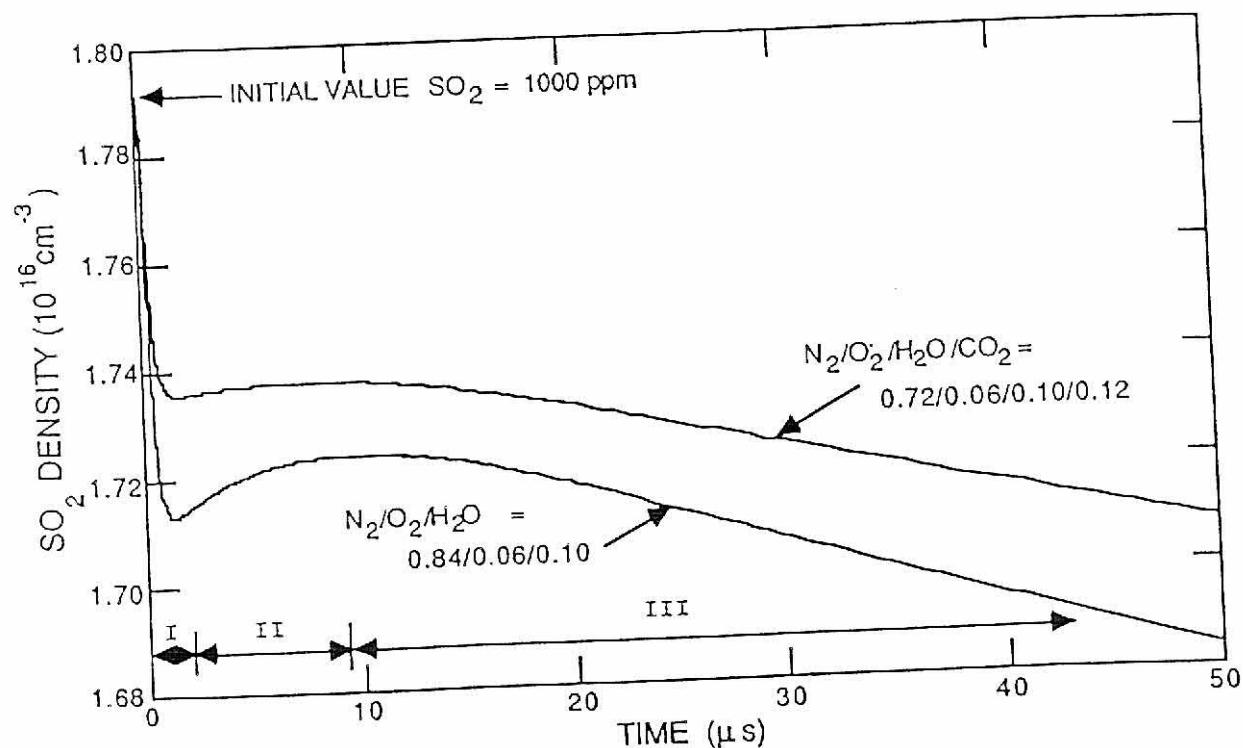


Figure 3.8 The density of SO_2 during and after a discharge pulse. The initial density is 1000 ppm. The initial depletion (Region I) is primarily due to reaction with $\text{N}_2(\text{A})$ forming the SO radical. This radical quickly oxidizes to form several products including SO_2 (Region II). SO_2 removal continues (Region III) by reaction with OH, HO_2 , and H_2O .

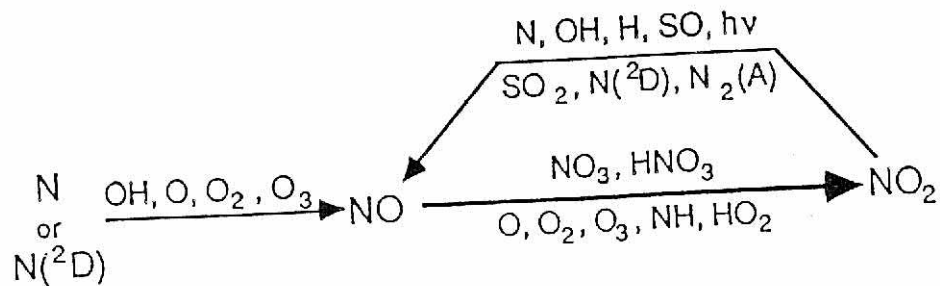


Figure 3.9 The primary reaction sequences in the formation and depletion of NO.

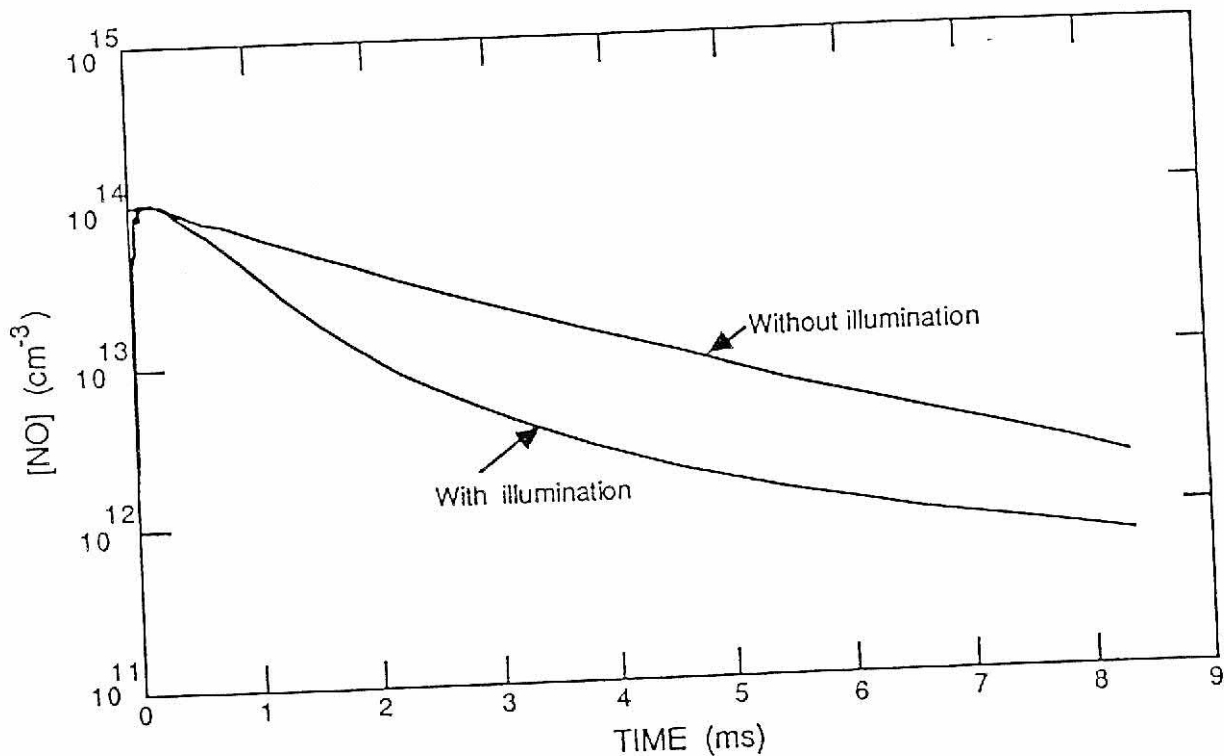


Figure 3.10 The density of NO during and after a discharge pulse in $\text{N}_2/\text{O}_2/\text{H}_2\text{O}/\text{CO}_2$ = 72/6/10/12 with and without illumination ($50 \text{ W}\cdot\text{cm}^{-2}$). The initial peak is approximately the same in both cases. Depletion occurs with either condition, but is more rapid with illumination.

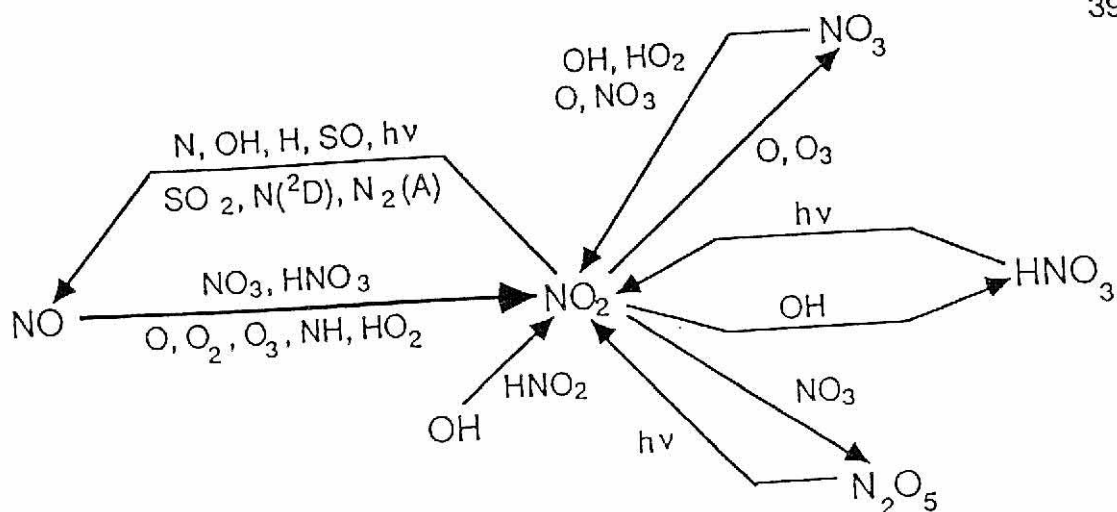


Figure 3.11 The primary reaction sequences in the formation and depletion of NO_2 .

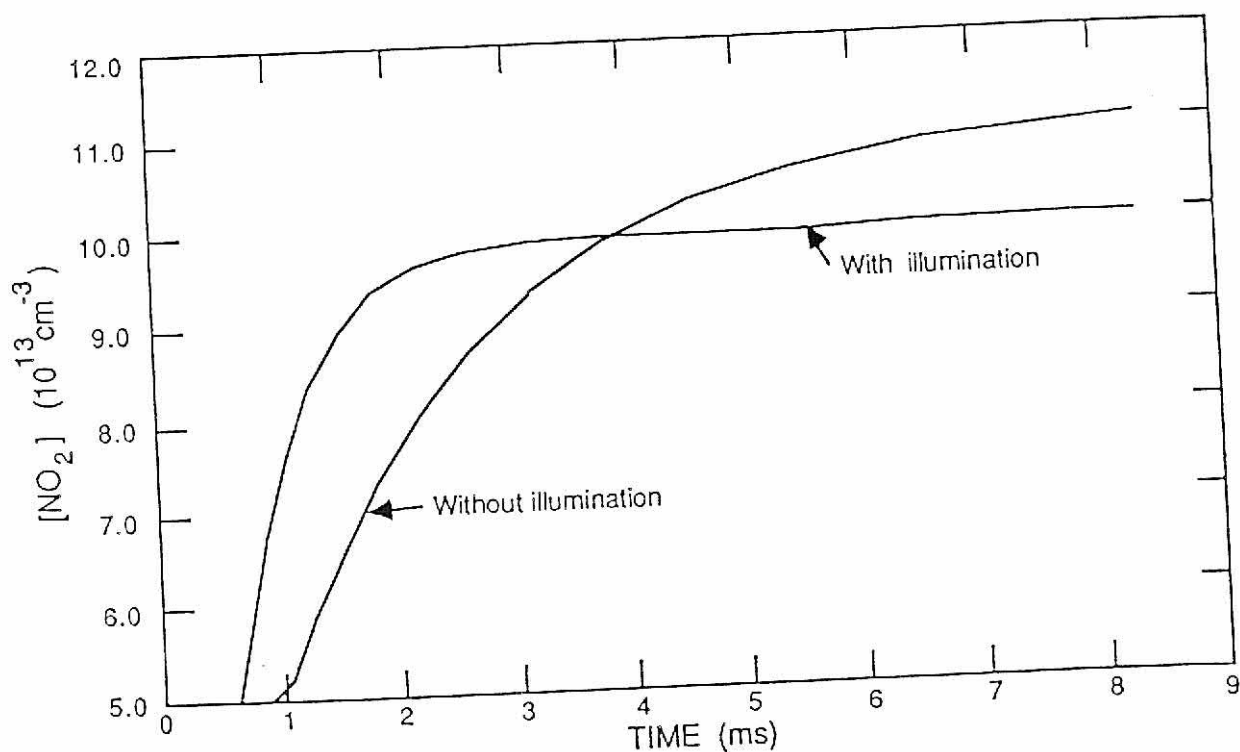


Figure 3.12 The density of NO_2 during and after a discharge pulse in $\text{N}_2/\text{O}_2/\text{H}_2\text{O}/\text{CO}_2 = 72/6/10/12$ with and without illumination (50 W-cm^{-2}). Without illumination, formation from NO is slower than with illumination. With illumination, a peak density is achieved and depletion slowly starts.

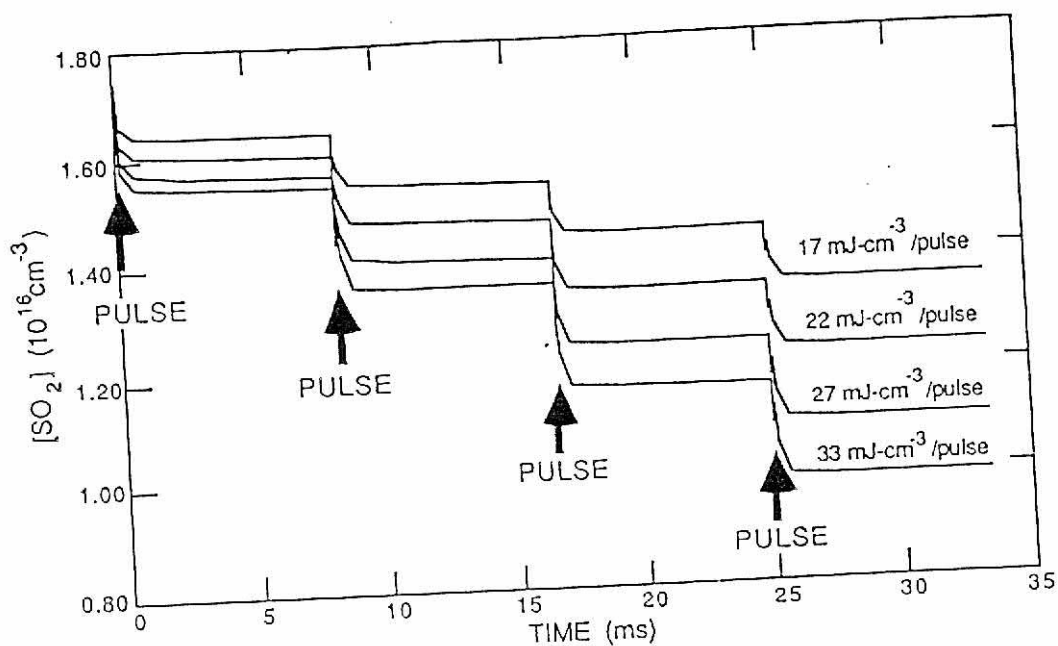


Figure 3.13 The density of SO_2 as a function of time using different energy depositions. The gas mixture is $\text{N}_2/\text{O}_2/\text{H}_2\text{O} = 84/6/10$. The initial density of SO_2 is 1000 ppm.

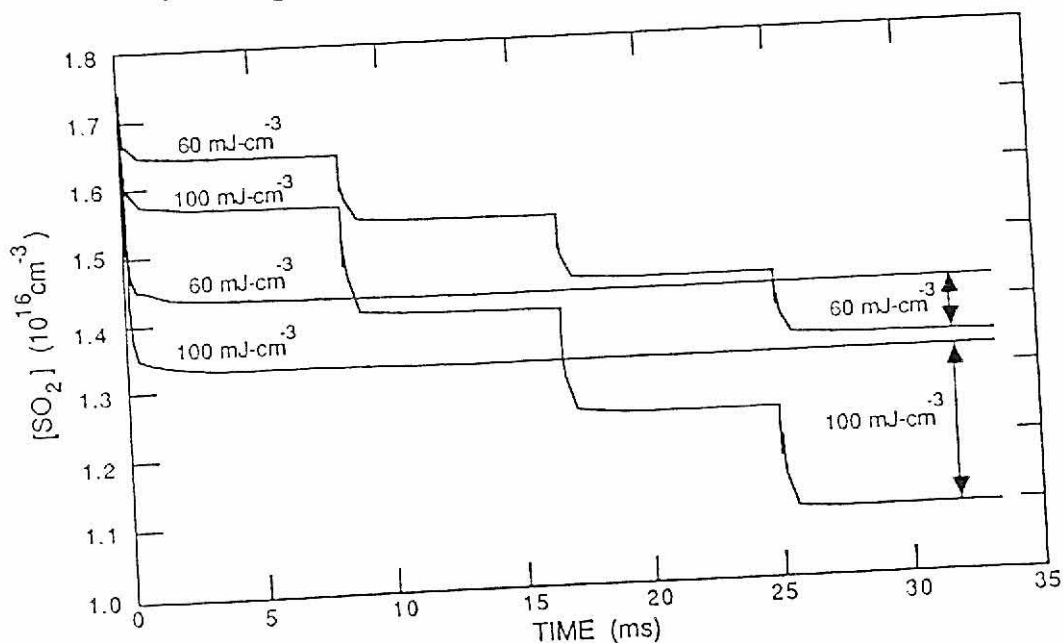


Figure 3.14 The density of SO_2 as a function of time using two different total energy depositions and two different types of energy depositions. The gas mixture is $\text{N}_2/\text{O}_2/\text{H}_2\text{O} = 84/6/10$. The initial density of SO_2 is 1000 ppm.

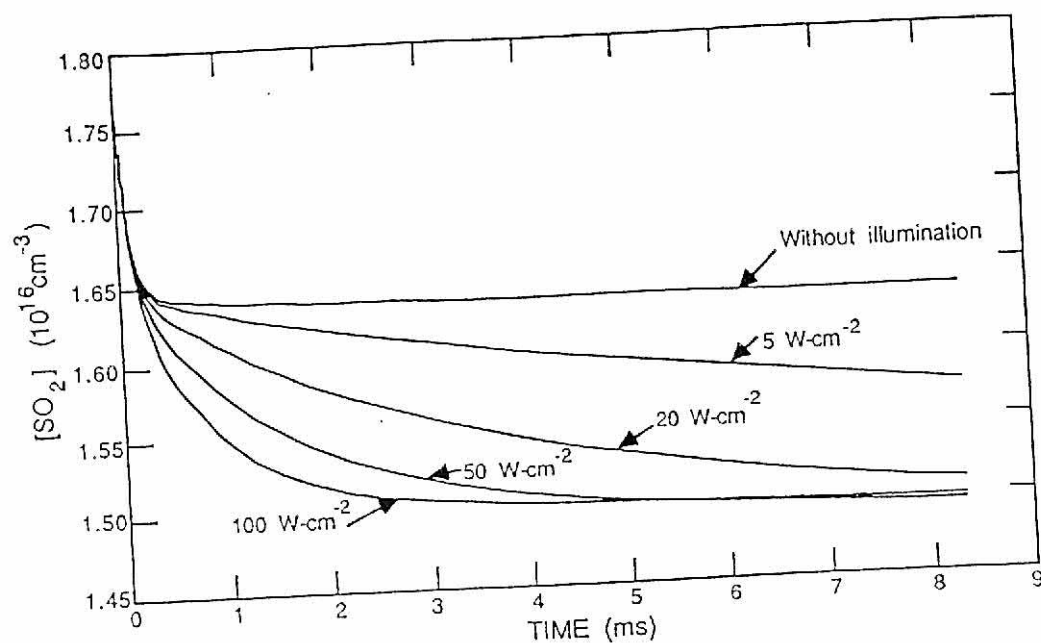


Figure 3.15 The density of SO_2 as a function of time and light intensity (0, 5, 20, 50, and 100 W-cm^{-2}). The gas mixture is $\text{N}_2/\text{O}_2/\text{H}_2\text{O}/\text{CO}_2 = 72/6/10/12$. The initial density of SO_2 is 1000 ppm.

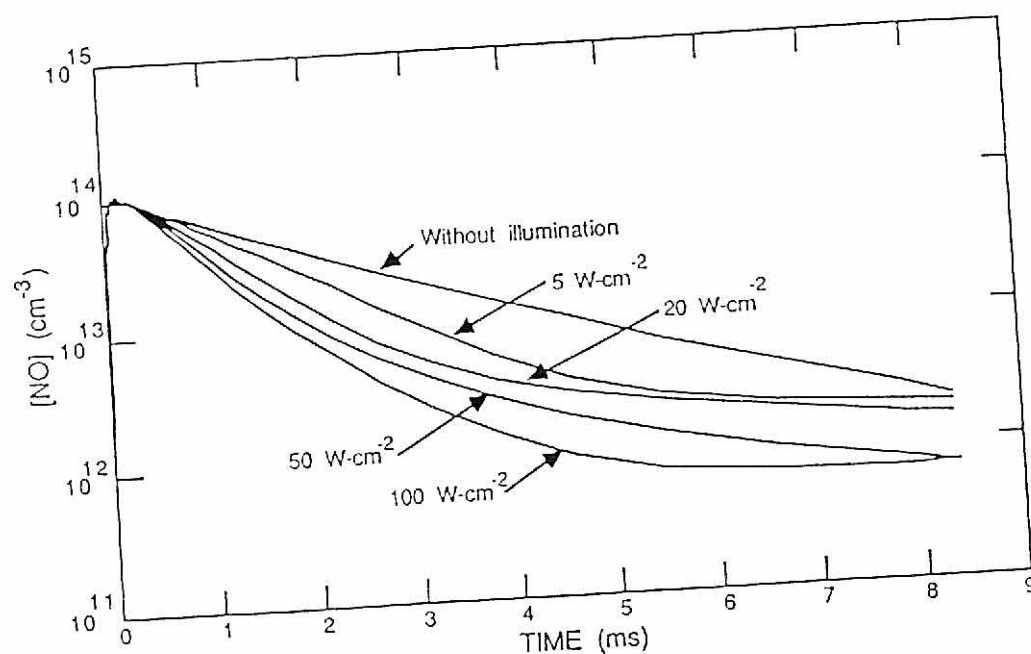


Figure 3.16 The density of NO as a function of time and light intensity (0, 5, 20, 50, and 100 W-cm^{-2}). The gas mixture is $\text{N}_2/\text{O}_2/\text{H}_2\text{O}/\text{CO}_2 = 72/6/10/12$.

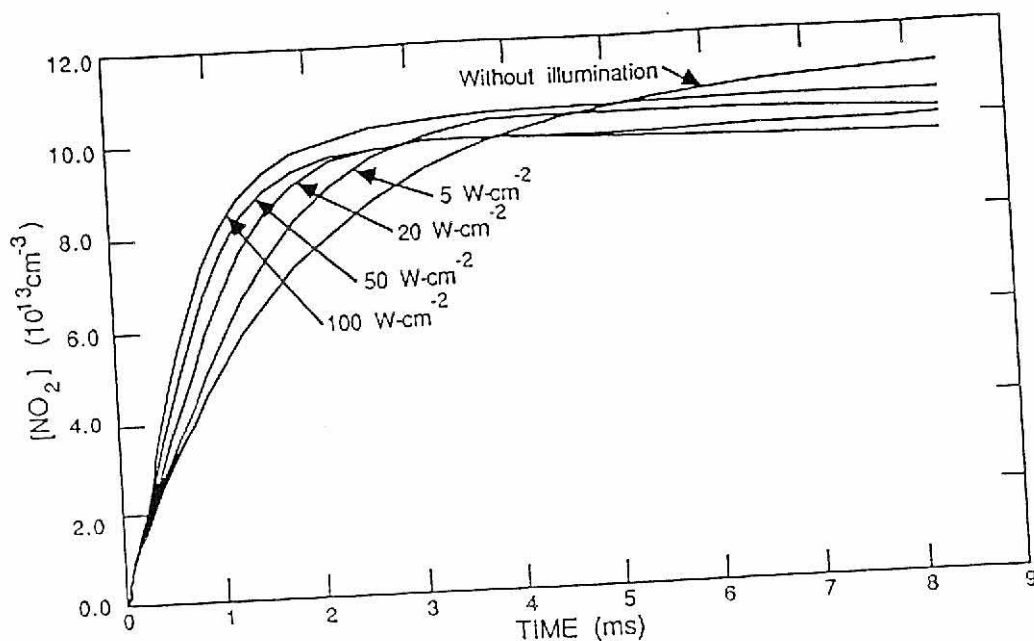


Figure 3.17 The density of NO_2 as a function of time and light intensity (0, 5, 20, 50, and 100 W-cm^{-2}). The gas mixture is $\text{N}_2/\text{O}_2/\text{H}_2\text{O}/\text{CO}_2 = 72/6/10/12$.

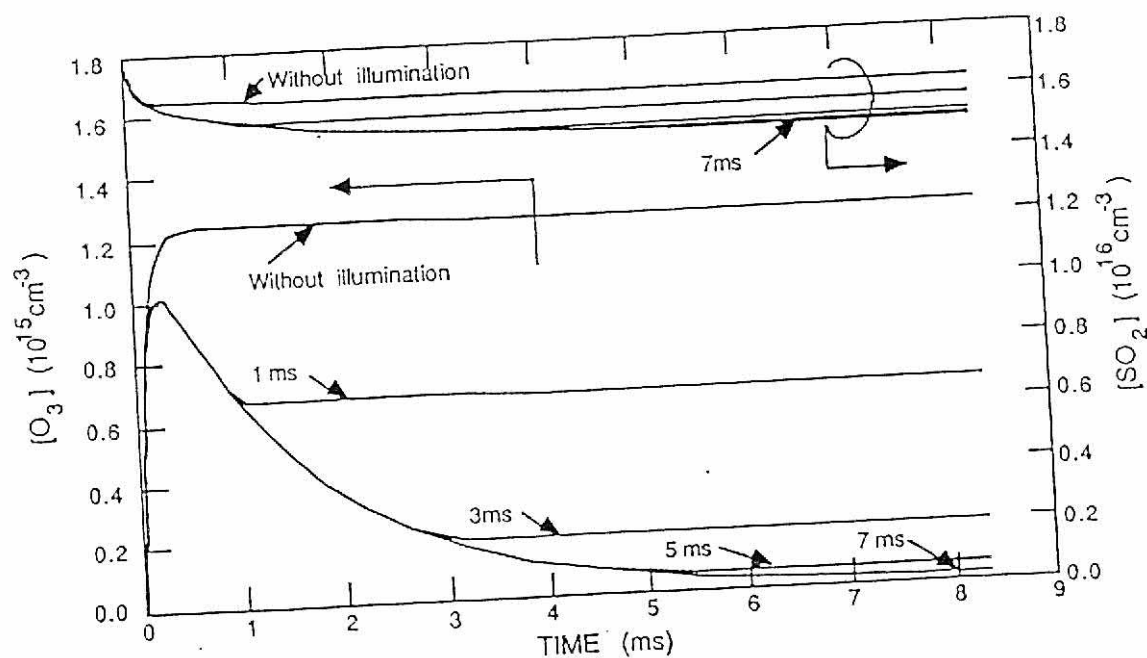


Figure 3.18 The densities of O_3 and SO_2 as a function of time using five different periods of light (0, 1, 3, 5, 7 ms). The light intensity is 50 W-cm^{-2} in all cases. The gas mixture is $\text{N}_2/\text{O}_2/\text{H}_2\text{O}/\text{CO}_2 = 72/6/10/12$.

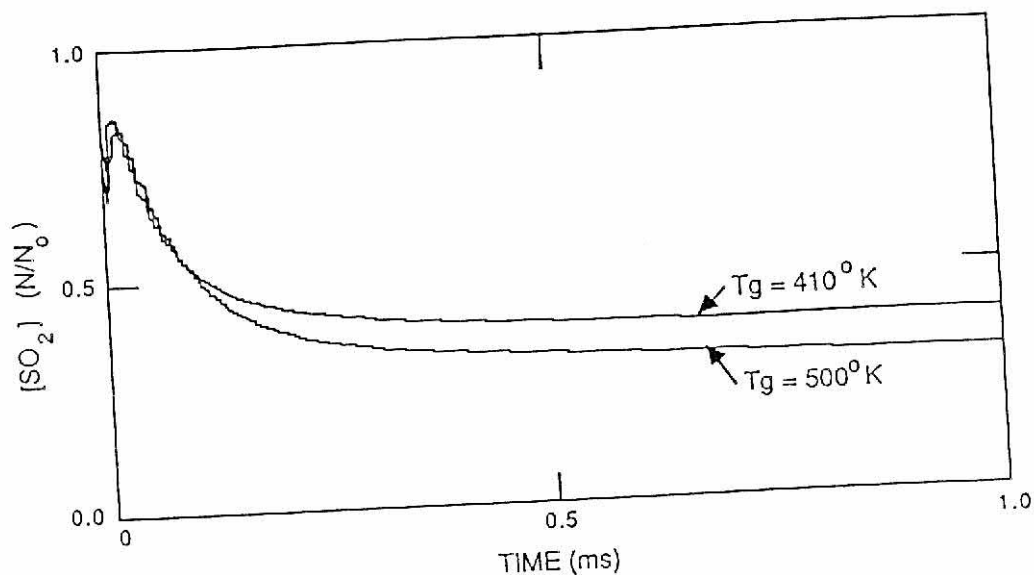


Figure 3.19 The normalized density of SO_2 as a function of time using two different initial gas temperatures (410°K and 500°K). Initial SO_2 density is 1000 ppm in each case. Gas mixture is $\text{N}_2/\text{O}_2/\text{H}_2\text{O} = 84/6/10$.

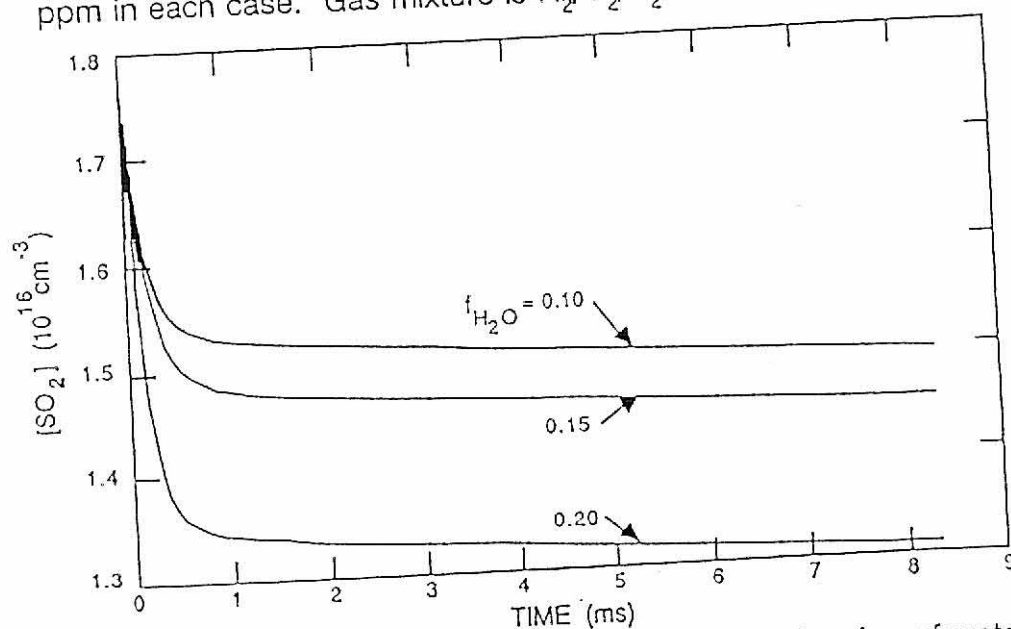


Figure 3.20 The density of SO_2 as a function of time and mole fraction of water in the gas mixture. The gas mixtures are $\text{N}_2/\text{O}_2/\text{H}_2\text{O}/\text{CO}_2 = 72.0/6.0/10.0/12.0$; $= 68.0/5.7/15.0/11.3$; $= 64.0/5.3/20.0/10.7$. The initial density of SO_2 is 1000 ppm.

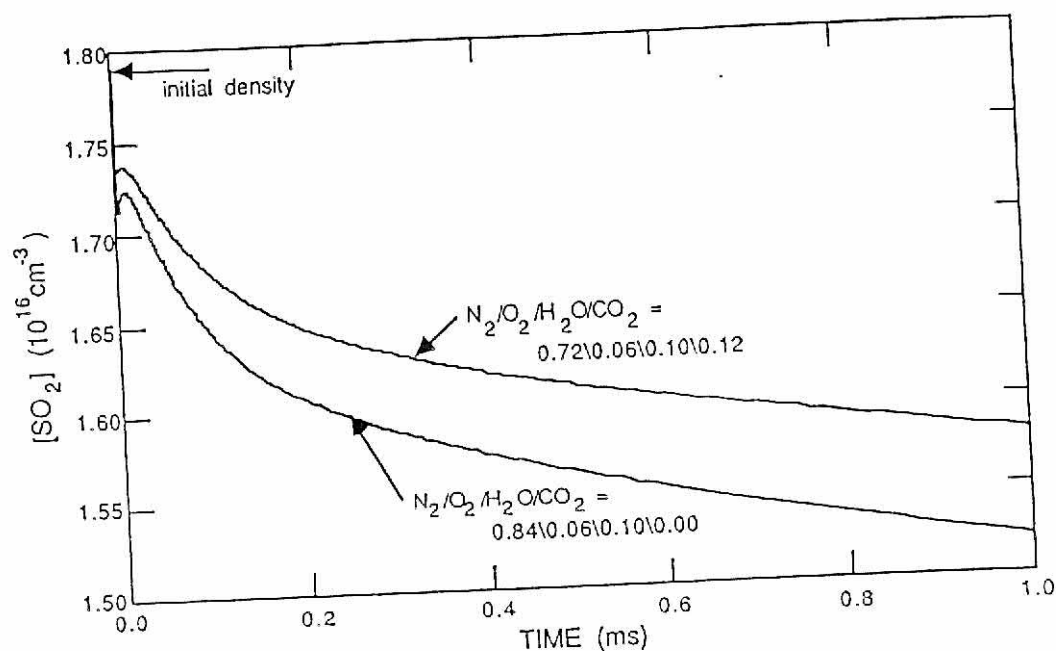


Figure 3.21 The density of SO_2 as a function of time and presence of CO_2 in the gas mixture. Initial density of SO_2 is 1000 ppm in both cases. Gas mixtures are $\text{N}_2/\text{O}_2/\text{H}_2\text{O}/\text{CO}_2 = 84/6/10/0$ and $72/6/10/12$.

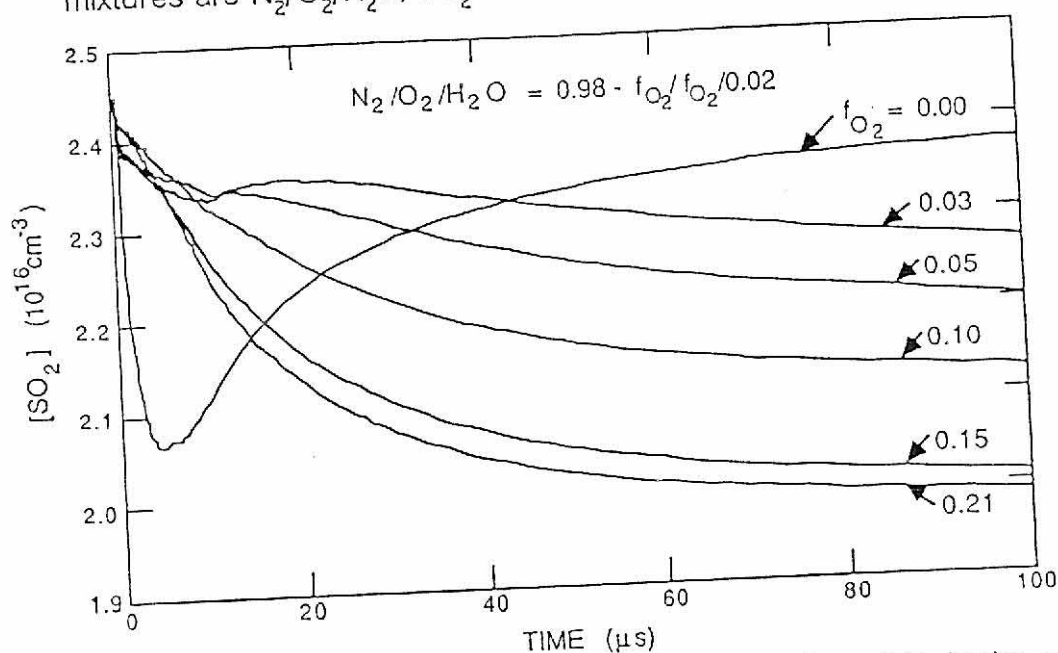


Figure 3.22 The density of SO_2 as a function of time and fraction of O_2 in the gas mixture. The initial density of SO_2 is 1000 ppm in all cases. The gas temperature is 300 °K.

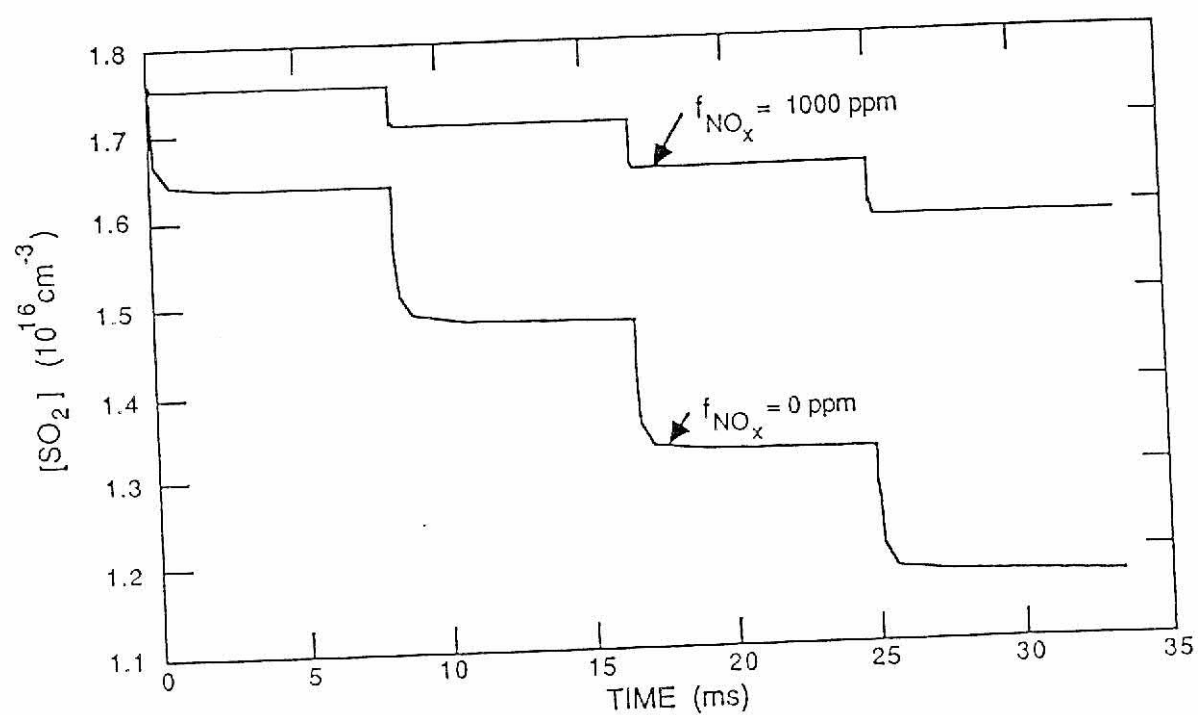


Figure 3.23 The density of SO₂ as a function of time and initial NO_x density. Initial SO₂ density is 1000 ppm in each case. For f_{NO_x} = 1000 ppm, the initial NO density = 500 ppm and the initial NO₂ = 500 ppm.

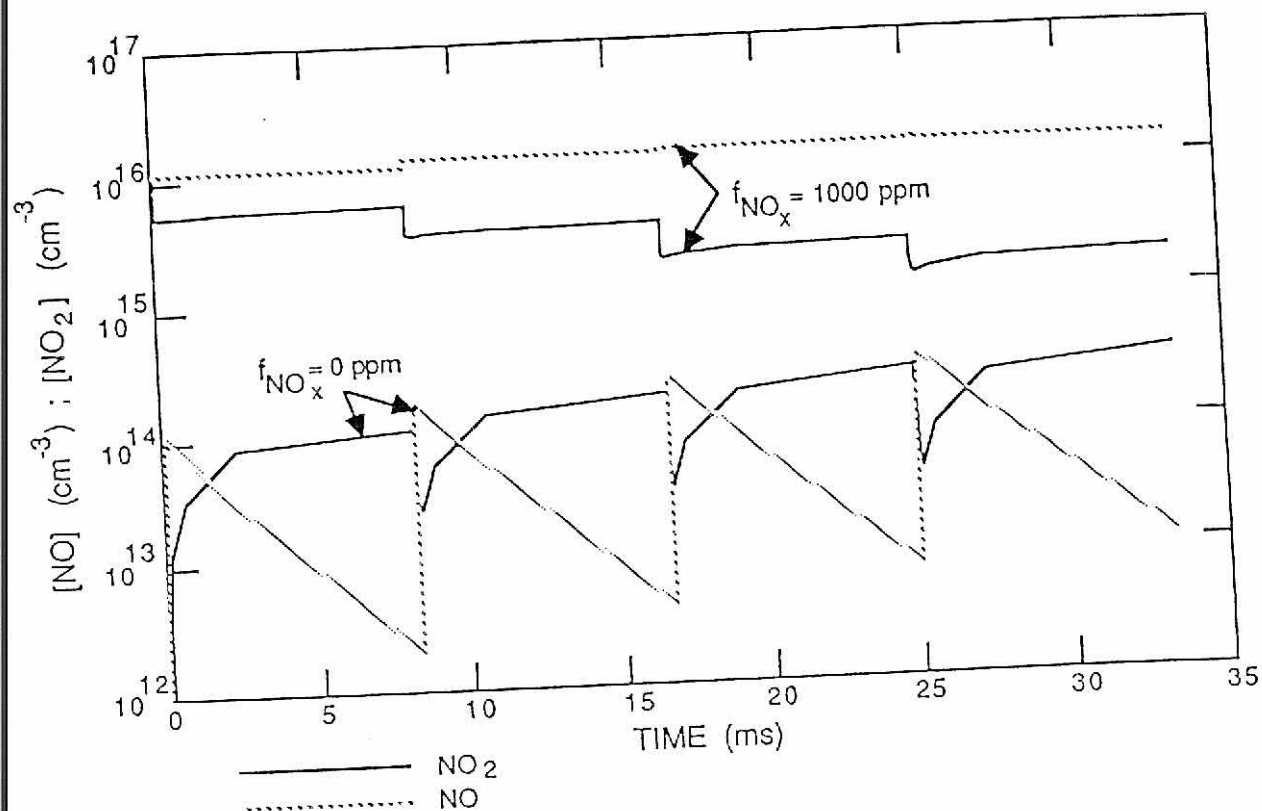


Figure 3.24 The densities of NO and NO₂ as a function of time and initial NO_x density. Initial SO₂ density is 1000 ppm. For $f_{\text{NO}_x} = 1000$ ppm, the initial NO density = 500 ppm and the initial NO₂ density = 500 ppm.

4. CONCLUSIONS

A comparison of results from the experimental setup with those results obtained by computer simulation verifies that the computer model accurately simulates the CPP process. Computer simulations of CPP can be used to predict removal results given a set of initial conditions or to optimize removal results based on initial gas compositions. The primary reaction pathways of the major species can be examined in detail.

The manner and amount of energy deposition are extremely important. A larger fractional amount of SO_2 is removed as more energy is used. However, the SO_2 removal efficiency and the total removal efficiency are increased if the energy is deposited in a series of small pulses rather than in one high energy pulse.

Optical processing increases the fractional amount of SO_2 removal, the SO_2 removal efficiency and the total removal efficiency. An optimum intensity can be calculated. Given a time period based on a 120 Hz excitation, increasing the intensity of light beyond the optimum intensity will not increase the fractional removal of SO_2 and will decrease the total removal efficiency.

As the gas temperature is increased, the fractional amount of SO_2 removal increases. Also, both removal efficiencies are enhanced by increasing the gas temperature in the range investigated.

The gas mixture in which CPP processing occurs affects the fractional amount of SO_2 removal and also the removal efficiencies. Addition of CO_2 to the gas mixture decreases the fractional amount of SO_2 removal but inhibits the generation of NO_x .

Both oxygen and water are necessary for the efficient removal of SO_2 and NO_x from the flue gas. A delicate balance between the amounts of O_2 and H_2O must be maintained to establish an efficient process.

If NO_x is initially present in the gas mixture, conditions must be established to inhibit the generation of NO_x and increase the removal of SO_2 and NO_x . The conditions which can be changed are gas mixture (including mole fractions of N_2 , O_2 , H_2O and CO_2), gas temperature, energy deposition and conditions of optical processing.

Once the concentration levels of SO_2 and NO_x have been determined and the gas mixture defined for a given system, the optimum parameters for removal may be found. This may include simple changes to the existing system such as the addition of water or other atmospheric species and the heating or cooling of the gas. The utilization of commercially available equipment makes CPP attractive to industry. Additional attractions are the low cost of construction and maintenance and the high safety factor. Therefore, combined plasma photolysis (CPP) is a practical and realistic method for the removal of SO_2 and NO_x from flue gases.

APPENDIX. SPECIES AND REACTIONS

49

<u>SPECIES</u>	<u>CHARGE</u>	<u>SPECIES</u>	<u>CHARGE</u>
e	-1	NO ⁺ *O ₂	1
N ₂	0	N ⁺	1
O ₂	0	N ₄ ⁺	1
H ₂ O	0	O ₂ ⁺ *H ₂ O	1
N ₂ ⁺	1	H ₃ O ⁺ *H ₂ O	1
O	0	H ₃ O ⁺ *(H ₂ O) _m	1
O ₃	0	(m+1)H ₂ O	0
O(¹ D)	0	CO ₂ ⁺	1
OH	0	H ₂ NO ⁺	1
hν	0	O ₂ ⁻	-1
SO ₂	0	NH ₃	0
HSO ₃	0	NH ₂	0
SO ₃	0	NH ₃ ⁺	1
HO ₂	0	NH ₄ ⁺	1
NO ₂	0	NO ⁺ *H ₂	1
NO	0	NO ⁺ *(H ₂ O) ₂	1
HNO ₂	0	NO ⁺ *(H ₂ O) ₃	1
H	0	HOCO	0
H ⁻	-1	HOCO*	0
HNO	0	CO*	0
NO ₃	0	HCO	0
N	0	H ₂ CO ₂	0
H ₂	0	HCHO	0
HSO ₃ *H ₂ O	0	CHO	0
N ₂ O	0	H ₂ CO	0
CO	0	C ₂ O ₂	0
CO ₂	0	N ₂ O ₄	0
HNO ₃	0	M	0
HO ₂ NO ₂	0	NO ₃ ⁻	-1
H ₂ SO ₄	0	O ⁻	-1
H ₂ O ₂	0	O ⁺	1
N ₂ O ₅	0	NO ₂ ⁻	-1
N(² D)	0	NO ₂ ⁺	1
N ₂ (A)	0	NO ₂ [±]	1
SO	0	N ₃ ⁺	1
NH	0	O ₂ ⁺	1
H ₂ O ⁺	1	H ₃ O ⁺	1

REFERENCES	REACTION	SAMPLE RATE ¹	RATE FORMULA
[27-35]	$e + N_2 \rightarrow N_2^+ + 2e$	7.158e-12	from rate table
[27-35]	$e + N_2 \rightarrow N + N^+ + 2e$	8.741e-16	from rate table
[27-35]	$e + N_2 \rightarrow N_2(A) + e$	4.992e-09	from rate table
[27-35]	$e + N_2 \rightarrow 2N + e$	2.921e-10	from rate table
[36,37]	$e + O_2 \rightarrow O^+ + O$	0.000e+00	from rate table
[36,37]	$e + O_2 \rightarrow O_2^+ + 2e$	2.711e-11	from rate table
[36,37]	$e + O_2 \rightarrow 2O + e$	6.774e-10	from rate table
[36,37]	$e + O_2 \rightarrow O^+ + O + 2e$	2.763e-13	from rate table
[36,37]	$e + O_2 \rightarrow O(^1D) + O + e$	4.778e-09	from rate table
[36,37]	$N_2^+ + e \rightarrow N(^2D) + N$	1.220e-07	$(2.0e-7)/T_e^{0.5}$
[18]	$e + H_2O \rightarrow H_2O^+ + 2e$	7.976e-12	from rate table
[38]	$e + H_2O \rightarrow H + OH + e$	6.806e-12	from rate table
[38]	$e + H_2O \rightarrow H^+ + OH$	1.673e-11	from rate table
[38]	$e + CO_2 \rightarrow CO_2^+ + 2e$	2.237e-11	from rate table
[39]	$e + CO_2 \rightarrow O^+ + CO$	5.533e-12	from rate table
[39]	$O + 2O_2 \rightarrow O_3 + O_2$	6.900e-34	$(6.9e-34)[T_{gas}/300]^{-1.25}$
[10]	$h\nu + O_3 \rightarrow O(^1D) + O_2 + h\nu$	1.150e-17	(1.15e-17)
[19,20]	$HO_2 + h\nu \rightarrow OH + O + h\nu$	2.200e-19	(2.2e-19)
[19,20]	$H_2O_2 + h\nu \rightarrow 2OH + h\nu$	7.000e-20	(7.0e-20)
[19,20]	$NO_2 + h\nu \rightarrow NO + O + h\nu$	1.700e-20	(1.7e-20)
[19,20]	$N_2O_5 + h\nu \rightarrow NO + NO_2 + h\nu$	3.360e-19	(3.36e-19)
[19,20]	$HNO_3 + h\nu \rightarrow OH + NO_2 + h\nu$	1.900e-20	(1.9e-20)

¹ Units of cm³/s for two-body reactions and cm⁶/s for three-body reactions for T_{gas} = 300 °K, E/N = 200 Td, or T_e = 2.7 eV in a gas mixture N₂/O₂/H₂O/CO₂ = 0.84/0.06/0.10/0.12.

REFERENCES	REACTION	SAMPLE RATE	RATE FORMULA
[19,20]	$\text{HO}_2\text{NO}_2 + h\nu \rightarrow \text{HO}_2 + \text{NO}_2 + h\nu$	3.640e-19	(3.64e-19)
[13]	$\text{SO}_2 + \text{OH} + \text{M} \rightarrow \text{HSO}_3 + \text{M}$	1.000e-31	(1.0e-31)[$T_{\text{gas}}/300$] ^{-1.5}
[10]	$\text{SO}_2 + \text{O} + \text{O}_2 \rightarrow \text{SO}_3 + \text{O}_2$	1.427e-33	(4.0e-32)[$\exp(-1000/T_{\text{gas}})$]
[13]	$\text{SO}_2 + \text{HO}_2 \rightarrow \text{SO}_3 + \text{OH}$	5.000e-19	(5.0e-19)[$T_{\text{gas}}/300$] ^{0.5}
[13]	$\text{SO}_2 + \text{NO}_2 \rightarrow \text{SO}_3 + \text{NO}$	2.000e-24	(2.0e-24)[$T_{\text{gas}}/300$] ^{0.5}
[13]	$\text{SO}_2 + \text{OH} + \text{H}_2\text{O} \rightarrow \text{HSO}_3^*\text{H}_2\text{O}$	8.300e-32	(8.3e-32)[$T_{\text{gas}}/300$] ^{-1.5}
[22]	$\text{SO}_2 + \text{N}_2(\text{A}) \rightarrow \text{N}_2 + \text{SO} + \text{O}$	3.000e-11	(3.0e-11)[$T_{\text{gas}}/300$] ^{0.5}
[13]	$\text{SO}_2 + \text{O} + \text{N}_2 \rightarrow \text{SO}_3 + \text{N}_2$	1.427e-33	(4.0e-32)[$\exp(-1000/T_{\text{gas}})$]
[10]	$\text{SO}_2 + \text{OH} + \text{M} \rightarrow \text{HSO}_3 + \text{M}$	3.000e-31	(3.0e-31)[$T_{\text{gas}}/300$] ^{-2.9}
[10]	$\text{SO} + \text{O}_2 \rightarrow \text{SO}_2 + \text{O}$	7.124e-17	(1.4e-13)[$\exp(-2275/T_{\text{gas}})$]
[10]	$\text{SO} + \text{SO}_3 \rightarrow 2 \text{SO}_2$	2.000e-15	(2.0e-15)[$T_{\text{gas}}/300$] ^{0.5}
[16]	$\text{SO} + \text{OH} \rightarrow \text{SO}_2 + \text{H}$	1.100e-10	(1.1e-10)[$T_{\text{gas}}/300$] ^{0.5}
[16]	$\text{SO} + \text{O} + \text{M} \rightarrow \text{SO}_2 + \text{M}$	8.800e-31	(8.8e-31)[$T_{\text{gas}}/300$] ^{-1.5}
[16]	$\text{SO} + \text{NO}_2 \rightarrow \text{SO}_2 + \text{NO}$	1.400e-11	(1.4e-11)[$T_{\text{gas}}/300$] ^{0.5}
[13]	$\text{SO} + \text{O}_3 \rightarrow \text{SO}_2 + \text{O}_2$	9.109e-14	(4.5e-12)[$\exp(-1170/T_{\text{gas}})$]
[10]	$\text{SO}_3 + \text{H}_2\text{O} + \text{M} \rightarrow \text{H}_2\text{SO}_4 + \text{M}$	3.500e-32	(3.5e-32)[$T_{\text{gas}}/300$] ^{-1.5}
[13]	$\text{SO}_3 + \text{H}_2\text{O} \rightarrow \text{H}_2\text{SO}_4$	5.700e-15	(5.70e-15)[$T_{\text{gas}}/300$] ^{0.5}
[17]	$\text{HSO}_3 + \text{O}_2 \rightarrow \text{HO}_2 + \text{SO}_3$	4.000e-13	(4.0e-13)[$T_{\text{gas}}/300$] ^{0.5}
[16]	$\text{HSO}_3 + \text{OH} + \text{M} \rightarrow \text{H}_2\text{SO}_4 + \text{M}$	4.000e-31	(4.0e-31)[$T_{\text{gas}}/300$] ^{-1.5}
[16]	$\text{N}(\text{D}) + \text{N}_2 \rightarrow \text{N} + \text{N}_2$	2.400e-14	(2.4e-14)[$T_{\text{gas}}/300$] ^{0.5}
[13]	$\text{N}(\text{D}) + \text{O}_2 \rightarrow \text{NO} + \text{O}$	6.800e-12	(6.8e-12)[$T_{\text{gas}}/300$] ^{0.5}
[13]	$\text{N}(\text{D}) + \text{NO} \rightarrow \text{N}_2 + \text{O}$	6.300e-11	(6.3e-11)[$T_{\text{gas}}/300$] ^{0.5}
[13]	$\text{N}(\text{D}) + \text{N}_2\text{O} \rightarrow \text{NO} + \text{N}_2$	2.600e-12	(2.6e-12)[$T_{\text{gas}}/300$] ^{0.5}
[13]	$\text{N}(\text{D}) + \text{NO}_2 \rightarrow \text{N}_2\text{O} + \text{O}$	1.500e-12	(1.5e-12)[$T_{\text{gas}}/300$] ^{0.5}
[13]	$\text{N}(\text{D}) + \text{NO}_2 \rightarrow 2 \text{NO}$	1.500e-12	(1.5e-12)[$T_{\text{gas}}/300$] ^{0.5}

REFERENCES	REACTION	SAMPLE RATE	RATE FORMULA
[13]	$N(^2D) + NH_3 \rightarrow NH + NH_2$	5.000e-11	$(5.0e-11)[T_{gas}/300]^{0.5}$
[13]	$N_2(A) + N_2 \rightarrow 2 N_2$	3.700e-16	$(3.7e-16)[T_{gas}/300]^{0.5}$
[13]	$N_2(A) + NO \rightarrow NO + N_2$	2.800e-11	$(2.8e-11)[T_{gas}/300]^{0.5}$
[13]	$N_2(A) + O_2 \rightarrow 2 O + N_2$	1.500e-12	$(1.5e-12)[T_{gas}/300]^{0.5}$
[13]	$N_2(A) + O_2 \rightarrow O_2 + N_2$	8.100e-13	$(8.1e-13)[T_{gas}/300]^{0.5}$
[13]	$N_2(A) + N_2O \rightarrow 2 N_2 + O$	1.400e-11	$(1.4e-11)[T_{gas}/300]^{0.5}$
[13]	$N_2(A) + NO_2 \rightarrow NO + O + N_2$	1.000e-12	$(1.0e-12)[T_{gas}/300]^{0.5}$
[13]	$N_2(A) + e \rightarrow N_2^+ + 2 e$	1.607e-09	$(2.2e-7)[\exp(-9.33/T_e)][1/(20+9.33/T_e) + \ln(1.25(1+(T_e/9.33)))]/(T_e^{0.5})(1+9.33/T_e)]$
[21]			
[13]	$N + NO_2 \rightarrow N_2O + O$	2.400e-12	$(2.4e-12)[T_{gas}/300]^{0.5}$
[13]	$N + NO_2 \rightarrow 2 NO$	6.000e-13	$(6.0e-13)[T_{gas}/300]^{0.5}$
[13]	$2 N + M \rightarrow N_2 + M$	3.900e-33	$(3.9e-33)[T_{gas}/300]^{-1.5}$
[10]	$N + OH \rightarrow NO + H$	5.045e-11	$(3.8e-11)[\exp(85/T_{gas})]$
[13]	$N + O + M \rightarrow NO + M$	3.900e-32	$(3.9e-32)[T_{gas}/300]^{-1.5}$
[10]	$N + O_2 \rightarrow NO + O$	9.595e-17	$(4.4e-12)[\exp(-3220/T_{gas})]$
[13]	$N + O_3 \rightarrow NO + O_2$	5.000e-16	$(5.0e-16)[T_{gas}/300]^{0.5}$
[10]	$2 NO + O_2 \rightarrow 2 NO_2$	1.931e-38	$(3.3e-39)[\exp(530/T_{gas})]$
[10]	$NO + HO_2 \rightarrow NO_2 + OH$	8.235e-12	$(3.7e-12)[\exp(240/T_{gas})]$
[10]	$NO + O + O_2 \rightarrow NO_2 + O_2$	8.600e-32	$(8.6e-32)[T_{gas}/300]^{-1.8}$
[10]	$NO + OH + M \rightarrow HNO_2 + M$	7.400e-31	$(7.4e-31)(T_{gas}/300)^{-2.4}$
[10]	$NO + H + M \rightarrow HNO + M$	3.400e-32	$(3.4e-32)[T_{gas}/300]^{-1.5}$
[13]	$NO + NO_3 \rightarrow 2 NO_2$	2.638e-11	$(1.6e-11)[\exp(150/T_{gas})]$
[10]	$NO + O_3 \rightarrow NO_2 + O_2$	4.600e-14	$(4.6e-14)[T_{gas}/300]^{0.5}$
[13]	$NO + N \rightarrow N_2 + O$	3.100e-11	$(3.1e-11)[T_{gas}/300]^{0.5}$
[10]	$NO_2 + O_3 \rightarrow NO_3 + O_2$	3.408e-17	$(1.2e-13)[\exp(-2450/T_{gas})]$

REFERENCES	REACTION	SAMPLE RATE	RATE FORMULA
[10]	$\text{NO}_2 + \text{NO}_3 + \text{M} \rightarrow \text{N}_2\text{O}_5 + \text{M}$	2.700e-30	$(2.7\text{e}-30)[T_{\text{gas}}/300]^{-3.4}$
[14]	$2 \text{NO}_2 + \text{N}_2 \rightarrow \text{N}_2\text{O}_4 + \text{N}_2$	1.400e-33	$(1.4\text{e}-33)[T_{\text{gas}}/300]^{-3.8}$
[13]	$2 \text{NO}_3 \rightarrow 2 \text{NO}_2 + \text{O}_2$	1.200e-15	$(1.2\text{e}-15)[T_{\text{gas}}/300]^{0.5}$
[14]	$\text{N}_2\text{O}_4 + \text{N}_2 \rightarrow 2 \text{NO}_2 + \text{N}_2$	5.738e-15	$(1.29\text{e}-5)[T_{\text{gas}}/300]^{-3.8}[\exp(-6460/T_{\text{gas}})]$
[13]	$\text{N}_2\text{O}_5 \rightarrow \text{NO}_2 + \text{NO}_3$	7.300e+01	(7.3e+01)
[13]	$\text{N}_2\text{O}_5 + \text{H}_2\text{O} \rightarrow 2 \text{HNO}_3$	5.000e-21	$(5.0\text{e}-21)[T_{\text{gas}}/300]^{0.5}$
[13]	$\text{NH} + \text{O}_2 \rightarrow \text{HNO} + \text{O}$	2.300e-13	$(2.3\text{e}-13)[T_{\text{gas}}/300]^{0.5}$
[13]	$\text{NH} + \text{NO} \rightarrow \text{N}_2\text{O} + \text{H}$	1.300e-12	$(1.3\text{e}-12)[T_{\text{gas}}/300]^{0.5}$
[10]	$\text{NH}_2 + \text{NO} \rightarrow \text{N}_2 + \text{H}_2\text{O}$	1.600e-11	$(1.6\text{e}-11)[T_{\text{gas}}/300]^{-1.5}$
[10]	$\text{NH}_2 + \text{NO}_2 \rightarrow \text{N}_2\text{O} + \text{H}_2\text{O}$	1.900e-11	$(1.9\text{e}-11)[T_{\text{gas}}/300]^{-2.2}$
[23]	$\text{NH}_2 + \text{O} \rightarrow \text{NH} + \text{OH}$	1.200e-11	$(1.2\text{e}-11)[T_{\text{gas}}/300]^{0.5}$
[23]	$\text{NH}_2 + \text{O} \rightarrow \text{HNO} + \text{H}$	7.600e-11	$(7.6\text{e}-11)[T_{\text{gas}}/300]^{0.5}$
[15]	$\text{NH}_2 + \text{H}_2 \rightarrow \text{NH}_3 + \text{H}$	2.895e-15	$(5.98\text{e}-12)[\exp(-2290/T_{\text{gas}})]$
[15]	$\text{NH}_3 + \text{H} \rightarrow \text{NH}_2 + \text{H}_2$	6.791e-16	$(1.35\text{e}-10)[\exp(-3660/T_{\text{gas}})]$
[26]	$\text{HNO}_3 + \text{NO} \rightarrow \text{HNO}_2 + \text{NO}_2$	7.372e-21	$(7.372\text{e}-21)[T_{\text{gas}}/300]^{0.5}$
[10]	$\text{O}(^1\text{D}) + \text{N}_2 \rightarrow \text{O} + \text{N}_2$	2.571e-11	$(1.8\text{e}-11)[\exp(107/T_{\text{gas}})]$
[13]	$\text{O}(^1\text{D}) + \text{O}_2 \rightarrow \text{O} + \text{O}_2$	3.800e-11	$(3.8\text{e}-11)[T_{\text{gas}}/300]^{0.5}$
[13]	$\text{O}(^1\text{D}) + \text{CO}_2 \rightarrow \text{O} + \text{CO}_2$	7.400e-11	$(7.4\text{e}-11)[T_{\text{gas}}/300]^{0.5}$
[13]	$\text{O}(^1\text{D}) + \text{H}_2\text{O} \rightarrow \text{O} + \text{H}_2\text{O}$	1.200e-11	$(1.2\text{e}-11)[T_{\text{gas}}/300]^{0.5}$
[13]	$\text{O}(^1\text{D}) + \text{H}_2\text{O} \rightarrow 2 \text{OH}$	2.200e-10	$(2.2\text{e}-10)[T_{\text{gas}}/300]^{0.5}$
[13]	$\text{O}(^1\text{D}) + \text{NH}_3 \rightarrow \text{NH}_2 + \text{OH}$	2.500e-10	$(2.5\text{e}-10)[T_{\text{gas}}/300]^{0.5}$
[11]	$\text{O}(^1\text{D}) + \text{H}_2\text{O} \rightarrow \text{H}_2 + \text{O}_2$	2.300e-12	$(2.3\text{e}-12)[T_{\text{gas}}/300]^{0.5}$
[11]	$\text{O}(^1\text{D}) + \text{H}_2 \rightarrow \text{OH} + \text{H}$	1.100e-10	$(1.1\text{e}-10)[T_{\text{gas}}/300]^{0.5}$
[13]	$\text{O} + \text{O}_2 + \text{H}_2\text{O} \rightarrow \text{O}_3 + \text{H}_2\text{O}$	2.900e-34	$(2.9\text{e}-34)[T_{\text{gas}}/300]^{-1.5}$
[10]	$\text{O} + \text{HO}_2 \rightarrow \text{OH} + \text{O}_2$	5.648e-11	$(2.9\text{e}-11)[\exp(200/T_{\text{gas}})]$

REFERENCES	REACTION	SAMPLE RATE	RATE FORMULA
[10]	$O + O_3 \rightarrow 2 O_2$	8.336e-15	$(8.0e-12)[\exp(-2060/T_{gas})]$
[10]	$O + NO_2 \rightarrow M + NO_3 + M$	9.000e-32	$(9.0e-32)[T_{gas}/300]^{-2.0}$
[10]	$O + NO_2 \rightarrow NO + O_2$	9.697e-12	$(6.5e-12)[\exp(120/T_{gas})]$
[13]	$O + NO_3 \rightarrow O_2 + NO_2$	1.000e-11	$(1.0e-11)[T_{gas}/300]^{0.5}$
[12]	$O + OH \rightarrow H + O_2$	3.319e-11	$(2.3e-11)[\exp(110/T_{gas})]$
[12]	$O + H_2O_2 \rightarrow OH + HO_2$	1.782e-15	$(1.4e-12)[\exp(-2000/T_{gas})]$
[11]	$O + H_2 \rightarrow OH + H$	3.876e-18	$(1.6e-11)[\exp(-4570/T_{gas})]$
[10]	$O + O_2 + N_2 \rightarrow O_3 + N_2$	6.200e-34	$(6.2e-34)[T_{gas}/300]^{-2.0}$
[10]	$O + NO + N_2 \rightarrow NO_2 + N_2$	1.000e-31	$(1.0e-31)[T_{gas}/300]^{-1.6}$
[24]	$O + H + M \rightarrow OH + M$	1.620e-32	$(1.62e-32)[T_{gas}/300]^{-1.5}$
[13]	$H + O_2 \rightarrow M + HO_2 + M$	4.800e-32	$(4.8e-32)[T_{gas}/300]^{-1.5}$
[13]	$H + OH + M \rightarrow H_2O + M$	4.300e-31	$(4.3e-31)[T_{gas}/300]^{-1.5}$
[13]	$2 H + M \rightarrow H_2 + M$	4.800e-33	$(4.8e-33)[T_{gas}/300]^{0.5}$
[13]	$H + NO_2 \rightarrow OH + NO$	8.000e-11	$(8.0e-11)[T_{gas}/300]^{0.5}$
[12]	$H + HO_2 \rightarrow 2 OH$	6.459e-11	$(2.8e-10)[\exp(-440/T_{gas})]$
[10]	$H + O_3 \rightarrow OH + O_2$	2.827e-11	$(1.4e-10)[\exp(-480/T_{gas})]$
[13]	$H + HNO \rightarrow H_2 + NO$	1.000e-11	$(1.0e-11)[T_{gas}/300]^{0.5}$
[12]	$H + HO_2 \rightarrow H_2 + O_2$	3.107e-12	$(1.1e-10)[\exp(-1070/T_{gas})]$
[11]	$H + HO_2 \rightarrow H_2O + OH$	9.400e-13	$(9.4e-13)[T_{gas}/300]^{0.5}$
[12]	$H + H_2O_2 \rightarrow H_2O + OH$	5.091e-14	$(4.0e-11)[\exp(-2000/T_{gas})]$
[12]	$H + H_2O_2 \rightarrow HO_2 + H_2$	1.296e-16	$(8.0e-11)[\exp(-4000/T_{gas})]$
[12]	$H + O_2 \rightarrow OH + O$	3.555e-22	$(2.8e-7)T_{gas}^{-0.9}[\exp(-8750/T_{gas})]$
[12]	$H_2 + O_2 \rightarrow H + HO_2$	1.325e-51	$(2.4e-10)[\exp(-28500/T_{gas})]$
[12]	$OH + CO \rightarrow CO_2 + H$	1.472e-13	$(1.12e-13)[\exp((0.00091)(T_{gas}))]$
[12]	$2 OH \rightarrow O + H_2O$	1.028e-12	$(3.5e-16)T_{gas}^{-1.4}[\exp(200/T_{gas})]$

REFERENCES	REACTION	SAMPLE RATE	RATE FORMULA
[10]	$\text{OH} + \text{NO}_2 \rightarrow \text{N}_2 + \text{HNO}_3 + \text{N}_2$	2.200e-30	$(2.2\text{e}-30)[T_{\text{gas}}/300]^{-2.9}$
[11]	$\text{OH} + \text{HNO}_3 \rightarrow \text{NO}_3 + \text{H}_2\text{O}$	1.309e-13	$(1.5\text{e}-14)[\exp(650/T_{\text{gas}})]$
[13]	$\text{OH} + \text{HNO} \rightarrow \text{H}_2\text{O} + \text{NO}$	7.000e-11	$(7.0\text{e}-11)[T_{\text{gas}}/300]^{0.5}$
[10]	$\text{OH} + \text{HNO}_2 \rightarrow \text{NO}_2 + \text{H}_2\text{O}$	4.906e-12	$(1.8\text{e}-11)[\exp(-390/T_{\text{gas}})]$
[12]	$\text{OH} + \text{HO}_2 \rightarrow \text{H}_2\text{O} + \text{O}_2$	8.000e-11	$(2.4\text{e}-8)/T_{\text{gas}}$
[11]	$\text{OH} + \text{O}_3 \rightarrow \text{HO}_2 + \text{O}_2$	6.778e-14	$(1.9\text{e}-12)[\exp(-1000/T_{\text{gas}})]$
[13]	$\text{OH} + \text{N}_2\text{O} \rightarrow \text{HNO} + \text{NO}$	3.800e-17	$(3.8\text{e}-17)[T_{\text{gas}}/300]^{0.5}$
[10]	$2 \text{OH} + \text{O}_2 \rightarrow \text{H}_2\text{O}_2 + \text{O}_2$	3.716e-15	$(6.9\text{e}-31)[T_{\text{gas}}/300]^{-0.8}$
[10]	$\text{OH} + \text{H}_2\text{O}_2 \rightarrow \text{H}_2\text{O} + \text{HO}_2$	1.701e-12	$(2.9\text{e}-12)[\exp(-160/T_{\text{gas}})]$
[11]	$\text{OH} + \text{NH}_3 \rightarrow \text{NH}_2 + \text{H}_2\text{O}$	1.603e-13	$(3.5\text{e}-12)[\exp(-925/T_{\text{gas}})]$
[10]	$\text{OH} + \text{NO}_2 \rightarrow \text{O}_2 + \text{HNO}_3 + \text{O}_2$	2.600e-30	$(2.6\text{e}-30)[T_{\text{gas}}/300]^{-2.9}$
[12]	$\text{OH} + \text{H}_2 \rightarrow \text{H}_2\text{O} + \text{H}$	7.021e-15	$(7.7\text{e}-12)[\exp(-2100/T_{\text{gas}})]$
[24]	$\text{OH} + \text{H} + \text{M} \rightarrow \text{H}_2\text{O} + \text{M}$	5.600e-31	$(5.60\text{e}-31)[T_{\text{gas}}/300]^{-1.5}$
[24]	$\text{OH} + \text{CO} + \text{M} \rightarrow \text{HOCO}^* + \text{M}$	6.200e-33	$(6.2\text{e}-33)[T_{\text{gas}}/300]^{-1.5}$
[25]	$\text{OH} + \text{NO}_3 \rightarrow \text{HO}_2 + \text{NO}_2$	2.600e-11	$(2.6\text{e}-11)[T_{\text{gas}}/300]^{0.5}$
[12]	$\text{OH} + \text{M} \rightarrow \text{O} + \text{H} + \text{M}$	4.371e-82	$(4.0\text{e}-9)[\exp(-50400/T_{\text{gas}})]$
[12]	$\text{OH} + \text{O}_2 \rightarrow \text{O} + \text{HO}_2$	1.605e-49	$(3.7\text{e}-11)[\exp(-26500/T_{\text{gas}})]$
[9]	$\text{OH} + \text{H} \rightarrow \text{O} + \text{H}_2$	9.262e-12	$(1.14\text{e}-12)T_{\text{gas}}^{0.67}[\exp(-518/T_{\text{gas}})]$
[10]	$\text{OH} + \text{NO}_2 + \text{H}_2\text{O} \rightarrow \text{HNO}_3 + \text{H}_2\text{O}$	2.200e-30	$(2.2\text{e}-30)(T_{\text{gas}}/300)^{-2.9}$
[12]	$\text{HO}_2 + \text{M} \rightarrow \text{H} + \text{O}_2 + \text{M}$	6.917e-74	$(2.0\text{e}-5)T_{\text{gas}}^{-1.18}[\exp(-24363/T_{\text{gas}})]$
[10]	$\text{HO}_2 + \text{NO}_2 + \text{N}_2 \rightarrow \text{HO}_2\text{NO}_2 + \text{N}_2$	1.500e-31	$(1.50\text{e}-31)(T_{\text{gas}}/300)^{-3.2}$
[11]	$\text{HO}_2 + \text{O}_3 \rightarrow \text{OH} + 2 \text{O}_2$	1.895e-15	$(1.4\text{e}-14)[\exp(-600/T_{\text{gas}})]$
[10]	$2 \text{HO}_2 + \text{M} \rightarrow \text{H}_2\text{O}_2 + \text{O}_2 + \text{M}$	4.983e-32	$(1.9\text{e}-33)[\exp(980/T_{\text{gas}})]$
[25]	$\text{HO}_2 + \text{NO}_3 \rightarrow \text{OH} + \text{NO}_2 + \text{O}_2$	3.600e-12	$(3.6\text{e}-12)[T_{\text{gas}}/300]^{0.5}$
[25]	$\text{HO}_2 + \text{NO}_3 \rightarrow \text{HNO}_3 + \text{O}_2$	9.200e-13	$(9.2\text{e}-13)[T_{\text{gas}}/300]^{0.5}$

REFERENCES	REACTION	SAMPLE RATE	RATE FORMULA
[12]	$\text{HO}_2 + \text{H}_2 \rightarrow \text{H}_2\text{O}_2 + \text{H}$	5.430e-30	$(5.0\text{e}-11)[\exp(-13100/T_{\text{gas}})]$
[12]	$\text{H}_2\text{O} + \text{H} \rightarrow \text{H}_2 + \text{OH}$	2.027e-25	$(1.03\text{e}-16)T_{\text{gas}}^{1.9}[\exp(-9265/T_{\text{gas}})]$
[12]	$\text{H}_2\text{O} + \text{O} \rightarrow 2 \text{OH}$	4.406e-24	$(7.6\text{e}-15)T_{\text{gas}}^{1.3}[\exp(-8605/T_{\text{gas}})]$
[24]	$\text{H}_2\text{O} + \text{CO}^* \rightarrow \text{H}_2 + \text{CO}_2$	8.300e-11	$(8.3\text{e}-11)[T_{\text{gas}}/300]^{0.5}$
[24]	$\text{H}_2\text{O} + \text{CO}^* \rightarrow \text{OH} + \text{HCO}$	8.300e-11	$(8.3\text{e}-11)[T_{\text{gas}}/300]^{0.5}$
[24]	$\text{H}_2\text{O} + \text{CO}^* \rightarrow \text{H}_2\text{O} + \text{CO}$	8.300e-11	$(8.3\text{e}-11)[T_{\text{gas}}/300]^{0.5}$
[18]	$(m+1)\text{H}_2\text{O} \rightarrow 3 \text{H}_2\text{O}$	1.000e+07	$(1.0\text{e}+7)$
[12]	$\text{H}_2\text{O}_2 + \text{O}_2 \rightarrow 2 \text{HO}_2$	1.003e-39	$(9.0\text{e}-11)[\exp(-20000/T_{\text{gas}})]$
[10]	$\text{HO}_2\text{NO}_2 + \text{N}_2 \rightarrow \text{HO}_2 + \text{NO}_2 + \text{N}_2$	1.669e-20	$(5.0\text{e}-6)[\exp(-10000/T_{\text{gas}})]$
[10]	$\text{HO}_2\text{NO}_2 + \text{O}_2 \rightarrow \text{HO}_2 + \text{NO}_2 + \text{O}_2$	1.202e-20	$(3.6\text{e}-6)[\exp(-10000/T_{\text{gas}})]$
[13]	$\text{H}_2\text{O}^+ + \text{H}_2\text{O} \rightarrow \text{H}_3\text{O}^+ + \text{OH}$	1.700e-09	$(1.7\text{e}-09)[T_{\text{gas}}/300]^{0.5}$
[13]	$\text{H}_2\text{O}^+ + \text{O}_2 \rightarrow \text{O}_2^+ + \text{H}_2\text{O}$	4.300e-10	$(4.3\text{e}-10)[T_{\text{gas}}/300]^{0.5}$
[9]	$\text{H}_2\text{O}^+ + \text{e} \rightarrow \text{OH} + \text{H}$	6.600e-06	$(6.60\text{e}-6)[T_e]^{-0.5}$
[9]	$\text{H}_2\text{O}^+ + \text{e} \rightarrow \text{O} + \text{H} + \text{H}$	2.880e-06	$(2.88\text{e}-6)[T_e]^{-0.5}$
[9]	$\text{H}_2\text{O}^+ + \text{e} \rightarrow \text{O} + \text{H}_2$	2.520e-06	$(2.52\text{e}-6)[T_e]^{-0.5}$
[18]	$\text{H}_2\text{O}^+ + \text{NO}_2 \rightarrow \text{H}_2\text{O} + \text{NO}_2$	2.000e-06	$(2.0\text{e}-6)[T_{\text{gas}}/300]^{-0.5}$
[18]	$\text{H}_2\text{O}^+ + \text{NO}_3 \rightarrow \text{H}_2\text{O} + \text{NO}_3$	2.000e-06	$(2.0\text{e}-6)[T_{\text{gas}}/300]^{-0.5}$
[18]	$\text{H}_2\text{O}^+ + \text{O}_2 \rightarrow \text{H}_2\text{O} + \text{O}_2$	2.000e-06	$(2.0\text{e}-6)[T_{\text{gas}}/300]^{-0.5}$
[18]	$\text{H}_2\text{O}^+ + \text{H} \rightarrow \text{H} + \text{H}_2\text{O}$	3.000e-06	$(3.0\text{e}-6)[T_{\text{gas}}/300]^{-0.5}$
[18]	$\text{H}_2\text{O}^+ + \text{O} \rightarrow \text{O} + \text{H}_2\text{O}$	3.000e-06	$(3.0\text{e}-6)[T_{\text{gas}}/300]^{-0.5}$
[18]	$\text{H}_3\text{O}^+ + \text{H} \rightarrow \text{H}_2 + \text{H}_2\text{O}$	3.000e-06	$(3.0\text{e}-6)[T_{\text{gas}}/300]^{-0.5}$
[18]	$\text{H}_3\text{O}^+ + \text{O} \rightarrow \text{OH} + \text{H}_2\text{O}$	3.000e-06	$(3.0\text{e}-6)[T_{\text{gas}}/300]^{-0.5}$
[18]	$\text{H}_3\text{O}^+ + \text{e} \rightarrow \text{H}_2\text{O} + \text{H}$	1.220e-07	$(2.0\text{e}-7)/T_e^{0.5}$
[18]	$\text{H}_3\text{O}^+ + \text{NO}_2 \rightarrow \text{H}_2\text{O} + \text{H} + \text{NO}_2$	2.000e-06	$(2.0\text{e}-6)[T_{\text{gas}}/300]^{-0.5}$
[18]	$\text{H}_3\text{O}^+ + \text{NO}_3 \rightarrow \text{H}_2\text{O} + \text{H} + \text{NO}_3$	2.000e-06	$(2.0\text{e}-6)[T_{\text{gas}}/300]^{-0.5}$

REFERENCES	REACTION	SAMPLE RATE	RATE FORMULA
[18]	$\text{H}_3\text{O}^+ + \text{O}_2^- \rightarrow \text{H}_2\text{O} + \text{H} + \text{O}_2$	2.000e-06	$(2.0\text{e}-6)[\text{T}_{\text{gas}}/300]^{-0.5}$
[13]	$\text{H}_3\text{O}^+ + \text{H}_2\text{O} + \text{M} \rightarrow \text{H}_3\text{O}^{+*}\text{H}_2\text{O} + \text{M}$	5.000e-27	$(5.0\text{e}-27)[\text{T}_{\text{gas}}/300]^{-1.5}$
[13]	$\text{H}_3\text{O}^+ + \text{NH}_3 \rightarrow \text{NH}_4^+ + \text{H}_2\text{O}$	2.500e-09	$(2.5\text{e}-9)[\text{T}_{\text{gas}}/300]^{0.5}$
[18]	$\text{H}_3\text{O}^{+*}\text{H}_2\text{O} + \text{e}^- \rightarrow \text{H} + 2 \text{H}_2\text{O}$	1.220e-07	$(2.0\text{e}-7)/\text{T}_e^{0.5}$
[18]	$\text{H}_3\text{O}^{+*}\text{H}_2\text{O} + \text{NO}_2^- \rightarrow \text{H} + 2 \text{H}_2\text{O} + \text{NO}_2$	2.000e-06	$(2.0\text{e}-6)[\text{T}_{\text{gas}}/300]^{-0.5}$
[18]	$\text{H}_3\text{O}^{+*}\text{H}_2\text{O} + \text{NO}_3^- \rightarrow \text{H} + 2 \text{H}_2\text{O} + \text{NO}_3$	2.000e-06	$(2.0\text{E}-6)[\text{T}_{\text{gas}}/300]^{-0.5}$
[13]	$\text{H}_3\text{O}^{+*}\text{H}_2\text{O} + \text{H}_2\text{O} \rightarrow \text{H}_3\text{O}^{+*}(\text{H}_2\text{O})_m$	1.000e-09	$(1.0\text{e}-9)[\text{T}_{\text{gas}}/300]^{0.5}$
[18]	$\text{H}_3\text{O}^{+*}\text{H}_2\text{O} + \text{H}^- \rightarrow \text{H}_2 + 2 \text{H}_2\text{O}$	3.000e-06	$(3.0\text{e}-6)[\text{T}_{\text{gas}}/300]^{-0.5}$
[18]	$\text{H}_3\text{O}^{+*}\text{H}_2\text{O} + \text{O}^- \rightarrow \text{OH} + 2 \text{H}_2\text{O}$	3.000e-06	$(3.0\text{e}-6)[\text{T}_{\text{gas}}/300]^{-0.5}$
[18]	$\text{H}_3\text{O}^{+*}(\text{H}_2\text{O})_m + \text{e}^- \rightarrow \text{H} + (m+1)\text{H}_2\text{O}$	1.220e-07	$(2.0\text{e}-7)/\text{T}_e^{0.5}$
[13]	$\text{H}_3\text{O}^{+*}(\text{H}_2\text{O})_m + \text{NO}_2^- \rightarrow \text{H} + (m+1)\text{H}_2\text{O} + \text{NO}_2$	2.000e-07	$(2.0\text{e}-7)[\text{T}_{\text{gas}}/300]^{-0.5}$
[13]	$\text{H}_3\text{O}^{+*}(\text{H}_2\text{O})_m + \text{NO}_3^- \rightarrow \text{H} + (m+1)\text{H}_2\text{O} + \text{NO}_3$	2.000e-07	$(2.0\text{e}-7)[\text{T}_{\text{gas}}/300]^{-0.5}$
[18]	$\text{H}_3\text{O}^{+*}(\text{H}_2\text{O})_m + \text{O}_2^- \rightarrow \text{H} + (m+1)\text{H}_2\text{O} + \text{O}_2$	2.000e-06	$(2.0\text{e}-6)[\text{T}_{\text{gas}}/300]^{-0.5}$
[18]	$\text{H}_3\text{O}^{+*}(\text{H}_2\text{O})_m + \text{H}^- \rightarrow \text{H}_2 + (m+1)\text{H}_2\text{O}$	3.000e-06	$(3.0\text{e}-6)[\text{T}_{\text{gas}}/300]^{-0.5}$
[18]	$\text{H}_3\text{O}^{+*}(\text{H}_2\text{O})_m + \text{O}^- \rightarrow \text{OH} + (m+1)\text{H}_2\text{O}$	3.000e-06	$(3.0\text{e}-6)[\text{T}_{\text{gas}}/300]^{-0.5}$
[13]	$\text{N}^+ + \text{N}_2 + \text{M} \rightarrow \text{N}_3^+ + \text{M}$	5.200e-30	$(5.2\text{e}-30)[\text{T}_{\text{gas}}/300]^{-1.5}$
[13]	$\text{N}^+ + \text{O}_2 \rightarrow \text{NO}^+ + \text{O}$	2.600e-10	$(2.6\text{e}-10)[\text{T}_{\text{gas}}/300]^{0.5}$
[13]	$\text{N}^+ + \text{O}_2 \rightarrow \text{O}_2^+ + \text{N}$	3.100e-10	$(3.1\text{e}-10)[\text{T}_{\text{gas}}/300]^{0.5}$
[13]	$\text{N}^+ + \text{NO} \rightarrow \text{NO}^+ + \text{N}$	9.000e-10	$(9.0\text{e}-10)[\text{T}_{\text{gas}}/300]^{0.5}$
[13]	$\text{N}^+ + \text{NH}_3 \rightarrow \text{NH}_3^+ + \text{N}$	2.400e-09	$(2.4\text{e}-9)[\text{T}_{\text{gas}}/300]^{0.5}$
[13]	$\text{N}^+ + \text{O}_2 \rightarrow \text{O}^+ + \text{NO}$	3.600e-11	$(3.6\text{e}-11)[\text{T}_{\text{gas}}/300]^{0.52}$
[9]	$\text{N}^+ + \text{OH} \rightarrow \text{H}_2\text{O}^+ + \text{N}$	2.860e-09	$(5.55\text{e}-8)[\text{T}_{\text{gas}}]^{-0.52}$
[18]	$\text{N}^+ + \text{O}_2^- \rightarrow \text{N} + \text{O}_2$	2.000e-06	$(2.0\text{e}-6)[\text{T}_{\text{gas}}/300]^{-0.5}$
[18]	$\text{N}^+ + \text{NO}_2^- \rightarrow \text{N} + \text{NO}_2$	2.000e-06	$(2.0\text{e}-6)[\text{T}_{\text{gas}}/300]^{-0.5}$
[18]	$\text{N}^+ + \text{M} + \text{H}^- \rightarrow \text{NH} + \text{M}$	1.200e-25	$(1.2\text{e}-25)[\text{T}_{\text{gas}}/300]^{-1.5}$

REFERENCES	REACTION	SAMPLE RATE	RATE FORMULA
[18]	$N^+ + M \rightarrow O^+ + NO + M$	1.200e-25	$(1.2e-25)[T_{gas}/300]^{-1.5}$
[18]	$N^+ + NO_3^- \rightarrow N + NO_3$	2.000e-06	$(2.0e-6)[T_{gas}/300]^{-0.5}$
[13]	$N_2^+ + NO \rightarrow NO^+ + N_2$	3.300e-10	$(3.3e-10)[T_{gas}/300]^{0.5}$
[13]	$N_2^+ + NO_2 \rightarrow NO_2^+ + N_2$	3.000e-10	$(3.0e-10)[T_{gas}/300]^{0.5}$
[13]	$N_2^+ + NO_2 \rightarrow NO^+ + N_2O$	5.000e-11	$(5.0e-11)[T_{gas}/300]^{0.5}$
[13]	$N_2^+ + NO_3^- \rightarrow N_2 + NO_3$	3.000e-06	$(3.0e-6)[T_{gas}/300]^{-0.5}$
[13]	$N_2^+ + NO_2^- \rightarrow N_2 + NO_2$	3.000e-06	$(3.0e-6)[T_{gas}/300]^{-0.5}$
[13]	$N_2^+ + N_2 + M \rightarrow N_4^+ + M$	1.100e-24	$(1.1e-24)[T_{gas}/300]^{-1.5}$
[13]	$N_2^+ + O_2 \rightarrow O_2^+ + N_2$	5.100e-11	$(5.1e-11)[T_{gas}/300]^{0.5}$
[13]	$N_2^+ + NH_3 \rightarrow NH_3^+ + N_2$	1.900e-09	$(1.9e-9)[T_{gas}/300]^{0.5}$
[18]	$N_2^+ + H^- \rightarrow H + N_2$	3.000e-06	$(3.0e-6)[T_{gas}/300]^{-0.5}$
[18]	$N_2^+ + O^- \rightarrow O + N_2$	3.000e-06	$(3.0e-6)[T_{gas}/300]^{-0.5}$
[18]	$N_3^+ + H^- \rightarrow NH + N_2$	3.000e-06	$(3.0e-6)[T_{gas}/300]^{-0.5}$
[18]	$N_3^+ + O^- \rightarrow NO + N_2$	3.000e-06	$(3.0e-6)[T_{gas}/300]^{-0.5}$
[13]	$N_3^+ + O_2 \rightarrow NO^+ + N_2O$	3.600e-11	$(3.6e-11)[T_{gas}/300]^{0.5}$
[13]	$N_3^+ + O_2 \rightarrow NO_2^+ + N_2$	1.500e-11	$(1.5e-11)[T_{gas}/300]^{0.5}$
[13]	$N_3^+ + NO \rightarrow NO^+ + N + N_2$	1.400e-10	$(1.4e-10)[T_{gas}/300]^{0.5}$
[13]	$N_3^+ + NO_2 \rightarrow NO^+ + NO + N_2$	7.000e-11	$(7.0e-11)[T_{gas}/300]^{0.5}$
[13]	$N_3^+ + NO_2 \rightarrow NO_2^+ + N + N_2$	7.000e-11	$(7.0e-11)[T_{gas}/300]^{0.5}$
[13]	$N_3^+ + N_2O \rightarrow NO^+ + 2 N_2$	5.000e-11	$(5.0e-11)[T_{gas}/300]^{0.5}$
[18]	$N_3^+ + e^- \rightarrow N + N_2$	1.220e-07	$(2.0e-7)/T_e^{0.5}$
[13]	$N_3^+ + NO_2^- \rightarrow N + N_2 + NO_2$	2.000e-06	$(2.0e-6)[T_{gas}/300]^{-0.5}$
[13]	$N_3^+ + H_2O \rightarrow H_2NO^+ + N_2$	3.300e-10	$(3.3e-10)[T_{gas}/300]^{0.5}$
[13]	$N_3^+ + NH_3 \rightarrow NH_3^+ + N + N_2$	2.100e-09	$(2.1e-9)[T_{gas}/300]^{0.5}$
[18]	$N_3^+ + NO_3^- \rightarrow N_2 + N + NO_3$	2.000e-06	$(2.0e-6)[T_{gas}/300]^{-0.5}$

REFERENCES	REACTION	SAMPLE RATE	RATE FORMULA
[18]	$N_3^+ + O_2^- \rightarrow N_2 + N + O_2$	2.000e-06	$(2.0e-6)[T_{gas}/300]^{-0.5}$
[13]	$N_4^+ + NO \rightarrow NO^+ + 2 N_2$	1.800e-09	$(1.8e-9)[T_{gas}/300]^{0.5}$
[13]	$N_4^+ + NO_2 \rightarrow NO_2^+ + 2 N_2$	2.500e-10	$(2.5e-10)[T_{gas}/300]^{0.5}$
[13]	$N_4^+ + NO_2 \rightarrow NO^+ + N_2O + N_2$	5.000e-11	$(5.0e-11)[T_{gas}/300]^{0.5}$
[13]	$N_4^+ + O_2 \rightarrow O_2^+ + 2 N_2$	2.500e-10	$(2.5e-10)[T_{gas}/300]^{0.5}$
[18]	$N_4^+ + e \rightarrow 2 N_2$	1.220e-07	$(2.0e-7)/T_e^{0.5}$
[13]	$N_4^+ + NO_2^- \rightarrow NO_2 + 2 N_2$	3.000e-06	$(3.0e-6)[T_{gas}/300]^{-0.5}$
[13]	$N_4^+ + NO_3^- \rightarrow NO_3 + 2 N_2$	3.000e-06	$(3.0e-6)[T_{gas}/300]^{-0.5}$
[18]	$N_4^+ + O_2^- \rightarrow 2 N_2 + O_2$	2.000e-06	$(2.0e-6)[T_{gas}/300]^{-0.5}$
[18]	$N_4^+ + H^- \rightarrow H + 2 N_2$	3.000e-06	$(3.0e-6)[T_{gas}/300]^{-0.5}$
[18]	$N_4^+ + O^- \rightarrow O + 2 N_2$	3.000e-06	$(3.0e-6)[T_{gas}/300]^{-0.5}$
[13]	$NO^+ + e \rightarrow N(^2D) + O$	1.650e-07	$(2.7e-7)/T_e^{0.5}$
[13]	$NO^+ + e \rightarrow N + O(^1D)$	1.220e-07	$(2.0e-7)/T_e^{0.5}$
[13]	$NO^+ + NO_2^- \rightarrow NO + NO_2$	3.000e-06	$(3.0e-6)[T_{gas}/300]^{-0.5}$
[13]	$NO^+ + NO_3^- \rightarrow NO + NO_3$	3.000e-06	$(3.0e-6)[T_{gas}/300]^{-0.5}$
[13]	$NO^+ + O_2 + M \rightarrow NO^+O_2 + M$	3.000e-31	$(3.0e-31)[T_{gas}/300]^{-1.5}$
[13]	$NO^+ + H_2O + M \rightarrow NO^+H_2O + M$	1.600e-28	$(1.6e-28)[T_{gas}/300]^{-1.5}$
[18]	$NO^+ + O_2^- \rightarrow NO + O_2$	2.000e-06	$(2.0e-6)[T_{gas}/300]^{-0.5}$
[18]	$NO^+ + H^- \rightarrow M \rightarrow HNO + M$	1.200e-25	$(1.2e-25)[T_{gas}/300]^{-0.5}$
[18]	$NO^+ + O^- \rightarrow NO + O$	3.000e-06	$(3.0e-6)[T_{gas}/300]^{-0.5}$
[18]	$NO_2^+ + H^- \rightarrow M \rightarrow HNO_2 + M$	1.200e-25	$(1.2e-25)[T_{gas}/300]^{-1.5}$
[18]	$NO_2^+ + O^- \rightarrow NO_2 + O$	3.000e-06	$(3.0e-6)[T_{gas}/300]^{-0.5}$
[13]	$NO_2^+ + NO \rightarrow NO^+ + NO_2$	2.900e-10	$(2.9e-10)[T_{gas}/300]^{0.5}$
[18]	$NO_2^+ + e \rightarrow NO + O$	1.220e-07	$(2.0e-7)/T_e^{0.5}$
[18]	$NO_2^+ + e \rightarrow NO + O(^1D)$	1.220e-07	$(2.0e-7)/T_e^{0.5}$

REFERENCES	REACTION	SAMPLE RATE	RATE FORMULA
[13]	$\text{NO}_2^+ + \text{NO}_2^- \rightarrow 2 \text{NO}_2$	3.000e-06	$(3.0\text{e}-6) [\text{T}_{\text{gas}}/300]^{-0.5}$
[13]	$\text{NO}_2^+ + \text{NO}_3^- \rightarrow \text{NO}_2 + \text{NO}_3$	3.000e-06	$(3.0\text{e}-6) [\text{T}_{\text{gas}}/300]^{-0.5}$
[18]	$\text{NO}_2^+ + \text{O}_2^- \rightarrow \text{NO}_2 + \text{O}_2$	2.000e-06	$(2.0\text{e}-6) [\text{T}_{\text{gas}}/300]^{-0.5}$
[18]	$\text{H}_2\text{NO}^+ + \text{e}^- \rightarrow \text{H}_2\text{O} + \text{N}$	1.220e-07	$(2.0\text{e}-7) / \text{T}_e^{0.5}$
[13]	$\text{H}_2\text{NO}^+ + \text{NO}_2^- \rightarrow \text{H}_2\text{O} + \text{N} + \text{NO}_2$	2.000e-06	$(2.0\text{e}-6) [\text{T}_{\text{gas}}/300]^{-0.5}$
[13]	$\text{H}_2\text{NO}^+ + \text{NO}_3^- \rightarrow \text{H}_2\text{O} + \text{N} + \text{NO}_3$	2.000e-06	$(2.0\text{e}-6) [\text{T}_{\text{gas}}/300]^{-0.5}$
[18]	$\text{H}_2\text{NO}^+ + \text{O}_2^- \rightarrow \text{H}_2\text{O} + \text{N} + \text{O}_2$	2.000e-06	$(2.0\text{e}-6) [\text{T}_{\text{gas}}/300]^{-0.5}$
[18]	$\text{H}_2\text{NO}^+ + \text{H}^- \rightarrow \text{H}_2 + \text{HNO}$	3.000e-06	$(3.0\text{e}-6) [\text{T}_{\text{gas}}/300]^{-0.5}$
[18]	$\text{H}_2\text{NO}^+ + \text{O}^- \rightarrow \text{OH} + \text{HNO}$	3.000e-06	$(3.0\text{e}-6) [\text{T}_{\text{gas}}/300]^{-0.5}$
[13]	$\text{NO}_2^- + \text{HNO}_3 \rightarrow \text{NO}_3^- + \text{HNO}_2$	1.600e-09	$(1.6\text{e}-9) [\text{T}_{\text{gas}}/300]^{0.5}$
[13]	$\text{NO}_2^- + \text{NO}_2 \rightarrow \text{NO}_3^- + \text{NO}$	1.000e-13	$(1.0\text{e}-13) [\text{T}_{\text{gas}}/300]^{0.5}$
[13]	$\text{NO}_2^- + \text{N}_2\text{O} \rightarrow \text{NO}_3^- + \text{N}_2$	5.000e-13	$(5.0\text{e}-13) [\text{T}_{\text{gas}}/300]^{0.5}$
[13]	$\text{NO}_2^- + \text{N}_2\text{O}_5 \rightarrow \text{NO}_3^- + 2 \text{NO}_2$	7.000e-10	$(7.0\text{e}-10) [\text{T}_{\text{gas}}/300]^{0.5}$
[13]	$\text{NO}_2^- + \text{O}_3 \rightarrow \text{NO}_3^- + \text{O}_2$	1.200e-10	$(1.2\text{e}-10) [\text{T}_{\text{gas}}/300]^{0.5}$
[13]	$\text{NO}_2 + \text{e}^- \rightarrow \text{M} + \text{NO}_2^- + \text{M}$	9.790e-31	$(1.6\text{e}-30) / \text{T}_e^{0.5}$
[13]	$\text{NO}_3^- + \text{NO} \rightarrow \text{NO}_2^- + \text{NO}_2$	5.000e-13	$(5.0\text{e}-13) [\text{T}_{\text{gas}}/300]^{0.5}$
[13]	$\text{NO}^* \text{O}_2 + \text{NO}_2^- \rightarrow \text{NO} + \text{O}_2 + \text{NO}_2$	3.000e-06	$(3.0\text{e}-6) [\text{T}_{\text{gas}}/300]^{-0.5}$
[13]	$\text{NO}^* \text{O}_2 + \text{NO}_2^- \rightarrow \text{NO}_3 + \text{NO}_2$	2.000e-07	$(2.0\text{e}-7) [\text{T}_{\text{gas}}/300]^{-0.5}$
[13]	$\text{NO}^* \text{O}_2 + \text{NO}_3^- \rightarrow \text{NO} + \text{O}_2 + \text{NO}_3$	3.000e-06	$(3.0\text{e}-6) [\text{T}_{\text{gas}}/300]^{-0.5}$
[18]	$\text{NO}^* \text{O}_2 + \text{e}^- \rightarrow \text{NO} + \text{O}_2$	1.220e-07	$(2.0\text{e}-7) / \text{T}_e^{0.5}$
[18]	$\text{NO}^* \text{O}_2 + \text{O}_2^- \rightarrow \text{NO} + 2 \text{O}_2$	2.000e-06	$(2.0\text{e}-6) [\text{T}_{\text{gas}}/300]^{-0.5}$
[18]	$\text{NO}^* \text{O}_2 + \text{H}^- \rightarrow \text{HNO} + \text{O}_2$	3.000e-06	$(3.0\text{e}-6) [\text{T}_{\text{gas}}/300]^{-0.5}$
[18]	$\text{NO}^* \text{O}_2 + \text{O}^- \rightarrow \text{NO}_2 + \text{O}_2$	3.000e-06	$(3.0\text{e}-6) [\text{T}_{\text{gas}}/300]^{-0.5}$
[13]	$\text{NH}_3^+ + \text{NH}_3 \rightarrow \text{NH}_4^+ + \text{NH}_2$	2.200e-09	$(2.2\text{e}-9) [\text{T}_{\text{gas}}/300]^{0.5}$
[13]	$\text{NH}_3^+ + \text{NO}_3^- \rightarrow \text{NH}_3 + \text{NO}_3$	3.000e-06	$(3.0\text{e}-6) [\text{T}_{\text{gas}}/300]^{-0.5}$

REFERENCES	REACTION	SAMPLE RATE	RATE FORMULA
[18]	$\text{NH}_3^+ + e \rightarrow \text{NH}_2 + \text{H}$	1.220e-07	$(2.0\text{e}-7)/T_e^{0.5}$
[18]	$\text{NH}_3^+ + \text{NO}_2^- \rightarrow \text{NH}_3 + \text{NO}_2$	2.000e-06	$(2.0\text{e}-6)[T_{\text{gas}}/300]^{-0.5}$
[18]	$\text{NH}_3^+ + \text{NO}_3^- \rightarrow \text{NH}_3 + \text{NO}_3$	2.000e-06	$(2.0\text{e}-6)[T_{\text{gas}}/300]^{-0.5}$
[18]	$\text{NH}_3^+ + \text{O}_2^- \rightarrow \text{NH}_3 + \text{O}_2$	2.000e-06	$(2.0\text{e}-6)[T_{\text{gas}}/300]^{-0.5}$
[18]	$\text{NH}_3^+ + \text{H}^- \rightarrow \text{H} + \text{NH}_3$	3.000e-06	$(3.0\text{e}-6)[T_{\text{gas}}/300]^{-0.5}$
[18]	$\text{NH}_3^+ + \text{O}^- \rightarrow \text{O} + \text{NH}_3$	3.000e-06	$(3.0\text{e}-6)[T_{\text{gas}}/300]^{-0.5}$
[18]	$\text{NH}_4^+ + \text{H}^- \rightarrow \text{H}_2 + \text{NH}_3$	3.000e-06	$(3.0\text{e}-6)[T_{\text{gas}}/300]^{-0.5}$
[18]	$\text{NH}_4^+ + \text{O}^- \rightarrow \text{OH} + \text{NH}_3$	3.000e-06	$(3.0\text{e}-6)[T_{\text{gas}}/300]^{-0.5}$
[18]	$\text{NH}_4^+ + e \rightarrow \text{NH}_3 + \text{H}$	1.220e-07	$(2.0\text{e}-7)/T_e^{0.5}$
[18]	$\text{NH}_4^+ + \text{NO}_2^- \rightarrow \text{NH}_3 + \text{H} + \text{NO}_2$	2.000e-06	$(2.0\text{e}-6)[T_{\text{gas}}/300]^{-0.5}$
[18]	$\text{NH}_4^+ + \text{NO}_3^- \rightarrow \text{NH}_3 + \text{H} + \text{NO}_3$	2.000e-06	$(2.0\text{e}-6)[T_{\text{gas}}/300]^{-0.5}$
[18]	$\text{NH}_4^+ + \text{O}_2^- \rightarrow \text{NH}_3 + \text{H} + \text{O}_2$	2.000e-06	$(2.0\text{e}-6)[T_{\text{gas}}/300]^{-0.5}$
[18]	$\text{NH}_4^+ + \text{NO}_3^- \rightarrow \text{NH}_3 + \text{H} + \text{NO}_3$	3.000e-06	$(3.0\text{e}-6)[T_{\text{gas}}/300]^{-0.5}$
[13]	$\text{NO}^{*}\text{H}_2\text{O} + e \rightarrow \text{NO} + \text{H}_2\text{O}$	1.220e-07	$(2.0\text{e}-7)/T_e^{0.5}$
[18]	$\text{NO}^{*}\text{H}_2\text{O} + \text{NO}_2^- \rightarrow \text{NO} + \text{H}_2\text{O} + \text{NO}_2$	2.000e-06	$(2.0\text{e}-6)[T_{\text{gas}}/300]^{-0.5}$
[18]	$\text{NO}^{*}\text{H}_2\text{O} + \text{NO}_3^- \rightarrow \text{NO} + \text{H}_2\text{O} + \text{NO}_3$	2.000e-06	$(2.0\text{e}-6)[T_{\text{gas}}/300]^{-0.5}$
[18]	$\text{NO}^{*}\text{H}_2\text{O} + \text{O}_2^- \rightarrow \text{NO} + \text{H}_2\text{O} + \text{O}_2$	2.000e-06	$(2.0\text{e}-6)[T_{\text{gas}}/300]^{-0.5}$
[13]	$\text{NO}^{*}\text{H}_2\text{O} + \text{H}_2\text{O} + \text{M} \rightarrow \text{NO}^{*}(\text{H}_2\text{O})_2 + \text{M}$	1.000e-27	$(1.0\text{e}-27)[T_{\text{gas}}/300]^{-1.5}$
[18]	$\text{NO}^{*}\text{H}_2\text{O} + \text{H}^- \rightarrow \text{H} + \text{NO} + \text{H}_2\text{O}$	3.000e-06	$(3.0\text{e}-6)[T_{\text{gas}}/300]^{-0.5}$
[18]	$\text{NO}^{*}\text{H}_2\text{O} + \text{O}^- \rightarrow \text{O} + \text{NO} + \text{H}_2\text{O}$	3.000e-06	$(3.0\text{e}-6)[T_{\text{gas}}/300]^{-0.5}$
[18]	$\text{NO}^{*}(\text{H}_2\text{O})_2 + \text{H}^- \rightarrow \text{HNO} + 2 \text{H}_2\text{O}$	3.000e-06	$(3.0\text{e}-6)[T_{\text{gas}}/300]^{-0.5}$
[18]	$\text{NO}^{*}(\text{H}_2\text{O})_2 + \text{O}^- \rightarrow \text{NO}_2 + 2 \text{H}_2\text{O}$	3.000e-06	$(3.0\text{e}-6)[T_{\text{gas}}/300]^{-0.5}$
[13]	$\text{NO}^{*}(\text{H}_2\text{O})_2 + \text{M} \rightarrow \text{NO}^{*}\text{H}_2\text{O} + \text{H}_2\text{O} + \text{M}$	1.300e-12	$(1.3\text{e}-12)[T_{\text{gas}}/300]^{0.5}$
[13]	$\text{NO}^{*}(\text{H}_2\text{O})_2 + \text{H}_2\text{O} \rightarrow \text{NO}^{*}(\text{H}_2\text{O})_3$	1.000e-09	$(1.0\text{e}-9)[T_{\text{gas}}/300]^{0.5}$
[18]	$\text{NO}^{*}(\text{H}_2\text{O})_2 + e \rightarrow \text{NO} + 2 \text{H}_2\text{O}$	1.220e-07	$(2.0\text{e}-7)/T_e^{0.5}$

REFERENCES	REACTION	SAMPLE RATE	RATE FORMULA
[18]	$\text{NO}^*(\text{H}_2\text{O})_2 + \text{NO}_3^- \rightarrow \text{NO} + 2 \text{H}_2\text{O} + \text{NO}_3$	2.000e-06	$(2.0\text{e}-6)[\text{T}_{\text{gas}}/300]^{-0.5}$
[18]	$\text{NO}^*(\text{H}_2\text{O})_2 + \text{NO}_2^- \rightarrow \text{NO} + 2 \text{H}_2\text{O} + \text{NO}_2$	2.000e-06	$(2.0\text{e}-6)[\text{T}_{\text{gas}}/300]^{-0.5}$
[18]	$\text{NO}^*(\text{H}_2\text{O})_2 + \text{O}_2^- \rightarrow \text{NO} + 2 \text{H}_2\text{O} + \text{O}_2$	2.000e-06	$(2.0\text{e}-6)[\text{T}_{\text{gas}}/300]^{-0.5}$
[18]	$\text{NO}^*(\text{H}_2\text{O})_3 + \text{NO}_2^- \rightarrow \text{NO} + 3 \text{H}_2\text{O} + \text{NO}_2$	2.000e-06	$(2.0\text{e}-6)[\text{T}_{\text{gas}}/300]^{-0.5}$
[18]	$\text{NO}^*(\text{H}_2\text{O})_3 + \text{O}_2^- \rightarrow \text{NO} + 3 \text{H}_2\text{O} + \text{O}_2$	2.000e-06	$(2.0\text{e}-6)[\text{T}_{\text{gas}}/300]^{-0.5}$
[18]	$\text{NO}^*(\text{H}_2\text{O})_3 + \text{e}^- \rightarrow \text{NO} + 3 \text{H}_2\text{O}$	1.220e-07	$(2.0\text{e}-7)/\text{T}_e^{0.5}$
[18]	$\text{NO}^*(\text{H}_2\text{O})_3 + \text{NO}_3^- \rightarrow \text{NO} + 3 \text{H}_2\text{O} + \text{NO}_3$	2.000e-06	$(2.0\text{e}-6)[\text{T}_{\text{gas}}/300]^{-0.5}$
[18]	$\text{NO}^*(\text{H}_2\text{O})_3 + \text{H}_2\text{O} \rightarrow \text{H}_3\text{O}^{*+}(\text{H}_2\text{O})_m + \text{HNO}_2$	8.000e-11	$(8.0\text{e}-11)[\text{T}_{\text{gas}}/300]^{0.5}$
[13]	$\text{NO}^*(\text{H}_2\text{O})_3 + \text{H}^- \rightarrow \text{HNO} + 3 \text{H}_2\text{O}$	3.000e-06	$(3.0\text{e}-6)[\text{T}_{\text{gas}}/300]^{-0.5}$
[18]	$\text{NO}^*(\text{H}_2\text{O})_3 + \text{O}^- \rightarrow \text{NO}_2 + 3 \text{H}_2\text{O}$	3.000e-06	$(3.0\text{e}-6)[\text{T}_{\text{gas}}/300]^{-0.5}$
[18]	$\text{O}^* + \text{N}_2 \rightarrow \text{NO}^* + \text{N}$	1.200e-12	$(1.2\text{e}-12)[\text{T}_{\text{gas}}/300]^{0.5}$
[13]	$\text{O}^* + \text{NO} \rightarrow \text{NO}^* + \text{O}$	1.700e-12	$(1.7\text{e}-12)[\text{T}_{\text{gas}}/300]^{0.5}$
[13]	$\text{O}^* + \text{O}_2 \rightarrow \text{O}_2^* + \text{O}$	1.900e-11	$(1.9\text{e}-11)[\text{T}_{\text{gas}}/300]^{0.5}$
[13]	$\text{O}^* + \text{NO}_2 \rightarrow \text{NO}_2^* + \text{O}$	1.600e-09	$(1.6\text{e}-9)[\text{T}_{\text{gas}}/300]^{0.5}$
[13]	$\text{O}^* + \text{NO}_2^- \rightarrow \text{O} + \text{NO}_2$	2.000e-06	$(2.0\text{e}-6)[\text{T}_{\text{gas}}/300]^{-0.5}$
[13]	$\text{O}^* + \text{NO}_3^- \rightarrow \text{O} + \text{NO}_3$	2.000e-06	$(2.0\text{e}-6)[\text{T}_{\text{gas}}/300]^{-0.5}$
[18]	$\text{O}^* + \text{O}_2^- \rightarrow \text{O} + \text{O}_2$	2.000e-06	$(2.0\text{e}-6)[\text{T}_{\text{gas}}/300]^{-0.5}$
[18]	$\text{O}^* + \text{H}^- \rightarrow \text{M} \rightarrow \text{OH} + \text{M}$	1.200e-25	$(1.2\text{e}-25)[\text{T}_{\text{gas}}/300]^{-1.5}$
[18]	$\text{O}^* + \text{O}^- \rightarrow \text{M} \rightarrow \text{O}_2 + \text{M}$	1.200e-25	$(1.2\text{e}-25)[\text{T}_{\text{gas}}/300]^{-1.5}$
[18]	$\text{O}_2^* + \text{H}^- \rightarrow \text{M} \rightarrow \text{H}_2\text{O} + \text{M}$	1.200e-25	$(1.2\text{e}-25)[\text{T}_{\text{gas}}/300]^{-1.5}$
[18]	$\text{O}_2^* + \text{O}^- \rightarrow \text{O} + \text{O}_2$	3.000e-06	$(3.0\text{e}-6)[\text{T}_{\text{gas}}/300]^{-0.5}$
[18]	$\text{O}_2^* + \text{NO} \rightarrow \text{NO}^* + \text{O}_2$	4.400e-10	$(4.4\text{e}-10)[\text{T}_{\text{gas}}/300]^{0.5}$
[13]	$\text{O}_2^* + \text{NO}_2 \rightarrow \text{NO}_2^* + \text{O}_2$	8.800e-10	$(8.8\text{e}-10)[\text{T}_{\text{gas}}/300]^{0.5}$
[13]	$\text{O}_2^* + \text{NO}_2^- \rightarrow \text{O}_2 + \text{NO}_2$	2.000e-06	$(2.0\text{e}-6)[\text{T}_{\text{gas}}/300]^{-0.5}$
[13]	$\text{O}_2^* + \text{NO}_2 \rightarrow \text{O}_2 + \text{NO}_2$	1.200e-09	$(1.2\text{e}-9)[\text{T}_{\text{gas}}/300]^{0.5}$
[13]	$\text{O}_2^* + \text{H}_2\text{O} \rightarrow \text{H}_2\text{O} \rightarrow \text{H}_3\text{O}^* + \text{OH} + \text{O}_2$		

REFERENCES	REACTION	SAMPLE RATE	RATE FORMULA
[13]	$O_2^+ + H_2O + M \rightarrow O_2^+ \cdot H_2O + M$	2.500e-28	$(2.5e-28)[T_{gas}/300]^{-1.5}$
[13]	$O_2^+ + NH_3 \rightarrow NH_3^+ + O_2$	1.000e-09	$(1.0e-9)[T_{gas}/300]^{0.5}$
[18]	$O_2^+ + e + M \rightarrow O_2 + M$	4.900e-27	$(8.0e-27)/T_e^{0.5}$
[18]	$O_2^+ + NO_3 \rightarrow O_2 + NO_3$	2.000e-06	$(2.0e-6)[T_{gas}/300]^{-0.5}$
[18]	$O_2^+ + O_2 \rightarrow 2O_2$	2.000e-06	$(2.0e-6)[T_{gas}/300]^{-0.5}$
[13]	$O_2 + e + M \rightarrow O_2^+ + M$	6.120e-32	$(1.0e-31)/T_e^{0.5}$
[13]	$O_2^+ + NO_2 \rightarrow NO_2^+ + O_2$	7.000e-10	$(7.0e-10)[T_{gas}/300]^{0.5}$
[13]	$O_2^+ + N_2 \rightarrow N_2 + O_2$	2.000e-06	$(2.0e-06)[T_{gas}/300]^{-0.5}$
[18]	$O_2^+ \cdot H_2O + O_2 \rightarrow 2 O_2 + H_2O$	2.000e-06	$(2.0e-6)[T_{gas}/300]^{-0.5}$
[18]	$O_2^+ \cdot H_2O + NO_3 \rightarrow O_2 + NO_3 + H_2O$	2.000e-06	$(2.0e-6)[T_{gas}/300]^{-0.5}$
[18]	$O_2^+ \cdot H_2O + e \rightarrow O_2 + H_2O$	1.220e-07	$(2.0e-7)/T_e^{0.5}$
[18]	$O_2^+ \cdot H_2O + NO_2 \rightarrow O_2 + H_2O + NO_2$	2.000e-06	$(2.0e-6)[T_{gas}/300]^{-0.5}$
[18]	$O_2^+ \cdot H_2O + H \rightarrow HO_2 + H_2O$	3.000e-06	$(3.0e-6)[T_{gas}/300]^{-0.5}$
[18]	$O_2^+ \cdot H_2O + O \rightarrow O + O_2 + H_2O$	3.000e-06	$(3.0e-6)[T_{gas}/300]^{-0.5}$
[12]	$CO + O_2 \rightarrow CO_2 + O$	7.580e-47	$(4.2e-12)[\exp(-24000/T_{gas})]$
[12]	$CO + O + M \rightarrow CO_2 + M$	1.108e-35	$(1.7E-33)[\exp(-1510/T_{gas})]$
[12]	$CO + HO_2 \rightarrow OH + CO_2$	1.482e-27	$(2.5e-10)[\exp(-11900/T_{gas})]$
[12]	$CO_2 + H \rightarrow CO + OH$	1.394e-29	$(2.5e-10)[\exp(-13300/T_{gas})]$
[12]	$CO_2 + O \rightarrow CO + O_2$	1.215e-49	$(2.8e-11)[\exp(-26500/T_{gas})]$
[12]	$CHO + M \rightarrow H + CO + M$	5.616e-23	$(0.0085)T_{gas}^{-2.14}[\exp(-10278/T_{gas})]$
[12]	$CHO + H_2 \rightarrow HCHO + H$	2.774e-26	$(3.0e-18)T_{gas}^{2.0}[\exp(-8972/T_{gas})]$
[12]	$CHO + O \rightarrow H + CO_2$	5.000e-11	$(5.0e-11)[T_{gas}/300]^{0.5}$
[12]	$CHO + O \rightarrow OH + CO$	5.000e-11	$(5.0e-11)[T_{gas}/300]^{0.5}$
[12]	$HCO + O_2 \rightarrow HO_2 + CO$	4.999e-12	$(8.5e-11)[\exp(-850/T_{gas})]$
[12]	$HCO + H \rightarrow H_2 + CO$	2.000e-10	$(2.0e-10)[T_{gas}/300]^{0.5}$

<u>REFERENCES</u>	<u>REACTION</u>	<u>SAMPLE RATE</u>	<u>RATE FORMULA</u>
[12]	$\text{HCO} + \text{OH} \rightarrow \text{H}_2\text{O} + \text{CO}$	5.000e-11	$(5.0\text{e}-11)[T_{\text{gas}}/300]^{0.5}$
[12]	$\text{HCO} + \text{HO}_2 \rightarrow \text{OH} + \text{H} + \text{CO}_2$	5.000e-11	$(5.0\text{e}-11)[T_{\text{gas}}/300]^{0.5}$
[12]	$\text{HCO} + \text{H}_2\text{O}_2 \rightarrow \text{H}_2\text{CO} + \text{HO}_2$	1.527e-18	$(1.7\text{e}-13)[\exp(-3486/T_{\text{gas}})]$
[12]	$\text{HCO} + \text{H}_2\text{O} \rightarrow \text{H}_2\text{CO} + \text{OH}$	8.024e-32	$(3.9\text{e}-16)T_{\text{gas}}^{1.35}[\exp(-13146/T_{\text{gas}})]$
[12]	$2 \text{HCO} \rightarrow \text{H}_2\text{CO} + \text{CO}$	3.000e-11	$(3.0\text{e}-11)[T_{\text{gas}}/300]^{0.5}$
[12]	$2 \text{HCO} \rightarrow \text{H}_2 + 2\text{CO}$	5.000e-12	$(5.0\text{e}-12)[T_{\text{gas}}/300]^{0.5}$
[18]	$\text{CO}_2^+ + \text{e} \rightarrow \text{CO} + \text{O}$	1.220e-07	$(2.0\text{e}-7)/T_e^{0.5}$
[18]	$\text{CO}_2^+ + \text{NO}_2 \rightarrow \text{CO}_2 + \text{NO}_2$	2.000e-06	$(2.0\text{e}-6)[T_{\text{gas}}/300]^{-0.5}$
[18]	$\text{CO}_2^+ + \text{NO}_3 \rightarrow \text{CO}_2 + \text{NO}_3$	2.000e-06	$(2.0\text{e}-6)[T_{\text{gas}}/300]^{-0.5}$
[18]	$\text{CO}_2^+ + \text{O}_2 \rightarrow \text{CO}_2 + \text{O}_2$	2.000e-06	$(2.0\text{e}-6)[T_{\text{gas}}/300]^{-0.5}$
[13]	$\text{CO}_2^+ + \text{O}_2 \rightarrow \text{O}_2^+ + \text{CO}_2$	5.600e-11	$(5.6\text{e}-11)[T_{\text{gas}}/300]^{0.5}$
[13]	$\text{CO}_2^+ + \text{NO} \rightarrow \text{NO}^+ + \text{CO}_2$	1.200e-10	$(1.2\text{e}-10)[T_{\text{gas}}/300]^{0.5}$
[18]	$\text{CO}_2^+ + \text{H} \rightarrow \text{H} + \text{CO}_2$	3.000e-06	$(3.0\text{e}-6)[T_{\text{gas}}/300]^{-0.5}$
[18]	$\text{CO}_2^+ + \text{O} \rightarrow \text{O} + \text{CO}_2$	3.000e-06	$(3.0\text{e}-6)[T_{\text{gas}}/300]^{-0.5}$

REFERENCES

- [1] M. J. Rood and S. L. Kent, "Gas phase reaction methods for simultaneous SO₂ and NO_x removal from flue gases," *Report to Advanced Environmental Control Technology Research Center*, December 1987.
- [2] K. Kawamura and V. H. Shui, "Radiation treatment for removing SO₂ and NO_x from exhaust gases," *Proceedings of an International Conference on Industrial Application of Radioisotopes and Radiation Technology by the International Atomic Energy Agency*, Grenoble, France, (Sept. 1981), pp. 197-214, 1982.
- [3] B. J. Finlayson-Pitts and J. N. Pitts, Jr., *Atmospheric Chemistry: Fundamentals and Experimental Techniques*. New York: John Wiley & Sons, 1986, ch. 1.
- [4] R. H. Essenhigh, M. K. Misra, and D. W. Shaw, "Ignition of coal particles: a review," *Combustion and Flame*, vol. 77, pp. 3-30, 1989.
- [5] C. R. Ward, "Mineral matter in the Springfield-Harrisburg (No. 5) coal member in the Illinois basin," *Illinois State Geological Survey*, Circular 498, 1977.
- [6] R. D. Harvey, A. Kar, M. H. Bargh, and L. B. Kohlenberger, "Information system on chemistry of Illinois coal," *Final Report to the Coal Research Board*, Illinois Department of Energy and Natural Resources Through the Center for Research on Sulfur in Coal, State Geological Survey Division, 1985.
- [7] H. J. Gluskoter, R. R. Ruch, W. G. Miller, R. A. Cahill, G. B. Dreher, and J. K. Kuhn, "Trace elements in coal: occurrence and distribution," *Illinois State Geological Survey*, Circular 499, 1977.
- [8] W. L. Nighan, "Electron energy distributions and collision rates in electrically excited N₂, CO and CO₂," *Phys. Rev. A*, vol. 2, no. 5, pp. 1989-2000, 1970.
- [9] B. R. Rowe, F. Vallée, J. L. Queffelec, J. C. Gomet, and M. Morlais, "The yield of oxygen hydrogen atoms through dissociative recombination of H₂O⁺ ions with electrons," *J. Chem. Phys.*, vol. 88, pp. 845-850, 1988.
- [10] R. Atkinson, D. L. Baulch, R. A. Cox, R. F. Hampson, Jr., J. A. Kerr, and J. Troe, "Evaluated kinetic and photochemical data for atmospheric chemistry: supplement III," *Int. J. Chem. Kin.*, vol. 21, pp. 115-150, 1989.
- [11] S. Mukkavilli, C. K. Lee, K. Varghese, and L. L. Tavlarides, "Modeling of the electrostatic corona discharge reactor," *IEEE Trans. Plasma Sci.*, vol. 16, pp. 652-660, 1988.

- [12] W. Tsang and R. F. Hampson, "Chemical kinetic data base for combustion chemistry, Part I., methane and related compounds," *J. Phys. Chem. Ref. Data*, vol. 15, pp. 1087-1127, 1986.
- [13] J. C. Person and D. O. Ham, "Removal of SO_2 and NO_x from stack gases by electron beam irradiation," *Radiat. Phys. Chem.*, vol. 31, pp. 1-8, 1988.
- [14] P. Borrell, C. J. Cobos, and K. Luther, "Falloff curve and specific rate constants for the reaction $\text{NO}_2 + \text{NO}_2 \leftrightarrow \text{N}_2\text{O}_4$," *J. Phys. Chem.*, vol. 92, pp. 4377-4384, 1988.
- [15] W. Hack, P. Rouveiolles, and H. G. Wagner, "Direct measurements of the reactions $\text{NH}_2 + \text{H}_2 \leftrightarrow \text{NH}_3 + \text{H}$ at temperatures from 670 to 1000 K," *J. Phys. Chem.*, vol. 90, pp. 2505-2511, 1986.
- [16] F. Yin, D. Grosjean, and J. H. Seinfeld, "Analysis of atmospheric photooxidation mechanisms for organosulfur compounds," *J. Geophys. Res.*, vol. 91, pp. 14417-14438, 1986.
- [17] X. Wang, Y. G. Jin, M. Suto, L. C. Lee, and H. E. O'Neal, "Rate constant of the gas phase reaction of SO_3 with H_2O ," *J. Chem. Phys.*, vol. 89, pp. 4853-4860, 1988.
- [18] Estimate.
- [19] B. J. Finlayson-Pitts and J. N. Pitts, Jr., *Atmospheric Chemistry: Fundamentals and Experimental Techniques*. New York: John Wiley & Sons, 1986, pp. 405-580.
- [20] W. B. DeMore, M. J. Molina, S. P. Sander, D. M. Golden, R. F. Hampson, M. J. Kurylo, C. J. Howard, and A. R. Ravishankara, "Chemical kinetics and photochemical data for use in stratospheric modeling: evaluation number 8," *JPL Publication 87-41*, Jet Propulsion Laboratory, California Institute of Technology, Pasadena, California, 1987.
- [21] C. Deutsch, "Excitation and ionization of neutral atoms in a dense discharge," *J. Appl. Phys.*, vol. 44, pp. 1142-1145, 1973.
- [22] J. W. Gentry, H. R. Paur, H. Mätzing, and W. Baumann, "A modeling study on the dose rate effect on the efficiency of the EBDS-process (ES-VERFAHREN)," *Radiat. Phys. Chem.*, vol. 31, pp. 95-100, 1988.
- [23] H. Mätzing, "The kinetics of O atoms in the radiation treatment of waste gases," *Radiat. Phys. Chem.*, vol. 33, pp. 81-84, 1989.

- [24] R. K. Bera and R. J. Hanrahan, "Investigation of OH-H₂ and OH-CO reactions using argon-sensitized pulse radiolysis," *J. Appl. Phys.*, vol. 62, pp. 2523-2529, 1987.
- [25] A. Mellouki, G. Le Bras, and G. Poulet, "Kinetics of the reactions of NO₃ with OH and HO₂," *J. Phys. Chem.*, vol. 92, pp. 2229-2234, 1988.
- [26] R. Svensson and E. Ljungström, "A kinetic study of the decomposition of HNO₃ and its reaction with NO," *Int. J. Chem. Kin.*, vol. 20, pp. 857-866, 1988.
- [27] M. Hayashi, *Nagoya Institute of Technology Report No. IPPJ-AM-19*, 1981.
- [28] D. Rapp and P. Englander-Golden, "Total cross sections for ionization and attachment in gases by electron impact I. positive ionization," *J. Chem. Phys.*, vol. 43, no. 5, pp. 1464-1479, 1965.
- [29] A. G. Engelhardt, A. V. Phelps, and C. G. Risk, "Determination of momentum transfer and inelastic collision cross sections for electrons in nitrogen using transport coefficients," *Phys. Rev.*, vol. 135, no. 6A, pp. A1566-A1574, 1964.
- [30] A. V. Phelps and L. C. Pitchford, "Anisotropic scattering of electrons by N₂ and its effect on electron transport," *Phys. Rev. A*, vol. 31, no. 5, pp. 2932-2949, 1985.
- [31] G. J. Schulz, "Vibrational excitation of N₂, CO, and H₂ by electron impact," *Phys. Rev.*, vol. 135, no. 4A, pp. A988-A994, 1964.
- [32] D. Spence, J. L. Mauer, and G. J. Schulz, "Measurement of total inelastic cross sections for electron impact in N₂ and CO₂," *J. Chem. Phys.*, vol. 57, no. 12, pp. 5516-5521, 1972.
- [33] D. C. Cartwright, S. Trajmar, A. Chutjian, and W. Williams, "Electron impact excitation of the electronic states of N₂, II. Integral cross sections at incident energies from 10 to 50 eV," *Phys. Rev. A*, vol. 16, no. 3, pp. 1041-1051, 1977.
- [34] E. C. Zipf and R. W. McLaughlin, "On the dissociation of nitrogen by electron impact and by e.u.v. photo-absorption," *Planet. Space Science*, vol. 26, pp. 449 - 462, 1978.
- [35] W. L. Borst, "Excitation of several important metastable states of N₂ by electron impact," *Phys. Rev. A*, vol. 5, no. 2, pp. 648-656, 1972.
- [36] A. V. Phelps, "Tabulations of collision cross sections and calculated transport and reaction coefficients for electron collisions with O₂," *JILA Information Center Report No. 28*, University of Colorado, Boulder, Colorado, 1985.

- [37] H. Tawara and T. Kato, "Total and partial ionization cross sections of atoms and ions by electron impact," *Atomic Data and Nuclear Data Tables*, vol. 36, pp. 212-219, 1987.
- [38] M. Hayashi, "Electron collision cross-sections for molecules determined from beam and swarm data," *Swarm Studies and Inelastic Electron-Molecular Collisions*, L. C. Pitchford, B. V. McKoy, A. Chutjian, and S. Trajmar, Eds. New York: Springer-Verlag, 1987, p. 178.
- [39] J. J. Lowke, A. V. Phelps, and B. W. Irwin, "Predicted electron transport coefficients and operating characteristics of CO_2 - N_2 - He laser mixtures," *J. Appl. Phys.*, vol. 44, pp. 4664-4671, 1973.